5-12-2017

# Variable Patterns in Spur and Groove Reef Morphology Explained by Physical Controls and their Relevance for Platform-Top Sedimentology

Robert C. Gardiner Jr
*Nova Southeastern University*, rcgardiner.jr@gmail.com

HALMOS COLLEGE OF NATURAL SCIENCES AND OCEANOGRAPHY

# Variable Patterns in Spur and Groove Reef Morphology Explained by Physical Controls and their Relevance for Platform-Top Sedimentology

By

Robert Gardiner

Submitted to the Faculty of
Halmos College of Natural Sciences and Oceanography
in partial fulfillment of the requirements for
the degree of Masters of Science with a specialty in:

Marine Environmental Science

Nova Southeastern University

May 2017

Submitted in Partial Fulfillment of the Requirements for the Degree of

# Masters of Science:

# Marine Environmental Science

Robert Gardiner

Nova Southeastern University

Halmos College of Natural Sciences and Oceanography

May 2017

Committee Approval

_________________________________________

Dr. Sam Purkis, Major Advisor

_________________________________________

Dr. Bernhard Riegl, Committee Member

_________________________________________

Dr. Art Trembanis, Committee Member

## Acknowledgements

Many thanks to Dr. Sam Purkis for all your tremendous help and guidance through this endeavor. During my time in your lab, I learned how to become a better scientific writer, I came to understand the power of GIS and remote sensing in marine science, and you taught me the art of figure and map making. My growth in those regards is owed all to you; thank you.

Jeremy Kerr, Gwilym Rowlands, Alex Dempsey, Andrew Calhoun, Steve Saul, and Matt Jonhston- I wouldn't have been able to finish this project without all your selfless help and support. Thank you all for your unique inputs ranging from the development of computer codes used in this thesis to just how to navigate graduate school in general.

Dr. Riegl and Dr. Trembanis- thank you both for your input in shaping the scope of this thesis and for helping me focus on unique and novel ways to enhance my analysis.

Thank you to the Living Oceans Foundation and the Gale Foundation for allowing me the resources to complete this thesis.

## Abstract

Spur and groove (SaG) morphology is a common ornamentation of reef-armored Holocene carbonate platform margins. Composed of margin-normal promontories constructed of coral framestone, termed “spurs”, interleaved with similarly orientated gullies, “grooves”, this morphology varies based on a host of physical controls. Primarily, the surrounding oceanographic conditions as well as the size and shape of the platform the SaG is encompassing, directly influence the development and organization of SaG. Since grooves act as conduits for carbonate sediment transport, this study seeks to examine the relationship between SaG organization dictated by platform size and shape and how that in turn influences platform-top sedimentation. The analysis reveals trends that suggest platform shape plays a larger role than platform size in allowing highly organized SaG to develop on multiple margins around the platform. In turn, those trends would suggest these sites to have more stable platform top sediment deposits. However, many variables go in to the creation and maintenance of platform top cays. While this study enhanced the current understanding of how oceanographic conditions influence SaG development and organization, expanding on the concepts and results found in this study coupled with coring data of SaG and platform-top cays, could further link the connection between SaG and sediment transport.

**Key Words:** Spur and Groove, Carbonate platform, Fore Reef Slope, Reef Flat Zone, Precincts

# 1 Introduction

## 1.1 Aims of the thesis

It is with my selective, global-scale, study of nine reef sites (Figure 1) that I plan on exploring the relationship between spur and groove (SaG) morphology and the local oceanographic conditions that influence platform-top sedimentology. Therefore, the focus of this study is twofold. First, my aim is to enhance and expand the current understanding on the quantitative relationship between SaG morphology and the surrounding oceanographic conditions as well as the role platform size and shape plays in determining SaG development and organization. Second, is to investigate the influence of the SaG's spatial parameters and intrinsic patterns on sediment transport on and off the coral reef platform.

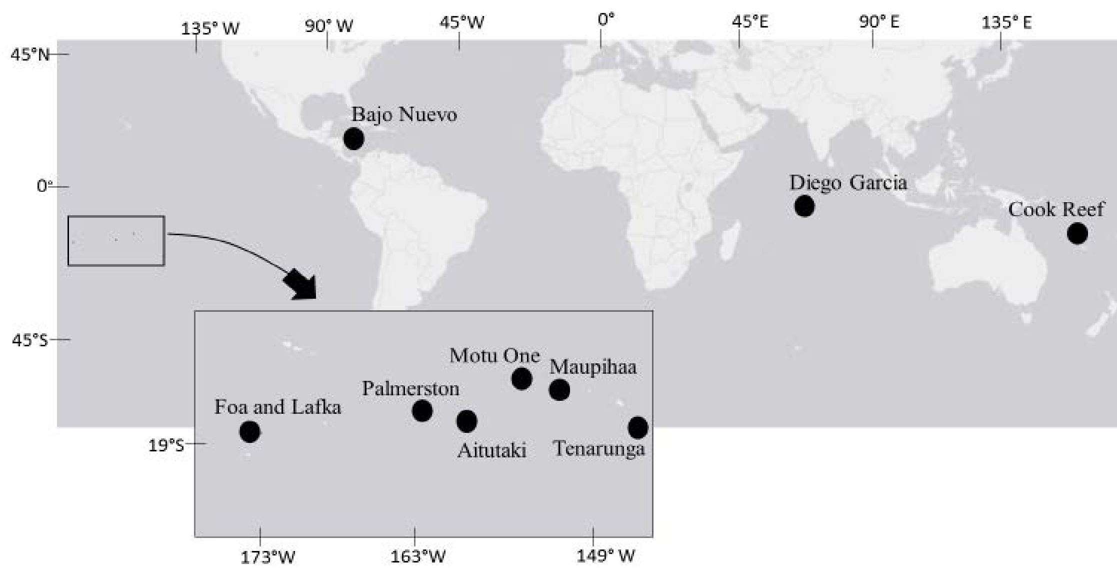


Figure 1. Locations of the nine sites investigated for this study. Left to Right: Foa and Lafuka Islands, Palmerston, Aitutaki, Motu One, Muahippa, Tenarunga, Bajo Nuevo, Diego Garcia, and Cook Reef.

## 1.2 What is spur and groove morphology

Spur and groove (SaG) morphology is a common ornamentation of reef-armored Holocene carbonate platform margins. This morphology is composed of margin-normal promontories constructed of coral framestone, termed "spurs", interleaved with similarly orientated gullies, "grooves" (Figure 2). While SaG morphology and its genesis have been previously examined (e.g. Munk and Sargent 1954; Shinn 1963, Sneh et al. 1980; Shinn et al. 1981, Kan et al. 1996; Blanchon 1997), further quantitative examination is warranted. Furthermore, high-resolution visible-spectrum satellite remote sensing, by virtue of its platform-scale coverage, provides a powerful tool to study the morphology. Remote sensing offers the opportunity to investigate several hitherto unexplained aspects of SaG geometry. For instance, the spacing and relief of spurs varies along different platform margins, as does the degree of development of the morphology. While the overall relationship between the physical processes and the tangible results expressed as SaG morphology have been observed, no robust quantitative correlations have been established. Conversely, there are certain aspects of SaG morphology which have been discussed in detail in the literature and are thus considered to be reasonably well-understood. Most notable of such observations are SaG mapping to a windward-leeward gradient and being more readily found in the high-energy zones of a platform (e.g. Shinn, 1963; Shinn et al., 1981; Blanchon, 1997). Variable patterns of spur and groove width have been reported in the literature to be linked to surrounding oceanographic conditions. The spacing of the spurs, termed their "periodicity", has also been considered in the context of sediment moving in the grooves. For instance, Kan et al. (1997) report that high rates of sediment flux serves to retard the lateral aggradation of spurs. The author informs that this effect serves to "tune (spur) growth longitudinally", along the principle axis of the spur. Because all off-platform sediment transport must pass through the SaG zone, there has been considerable interest in how the morphology impacts platform-scale sediment dynamics and the development of peri-platform slope deposits, in particular (e.g. Rogers et al. 2013). Through a modeling study, Rogers et al. (2013) shows that SaG formations can induce Lagrangian circulation patterns of onshore flow over the spurs and offshore flow through the grooves. In turn, this circulation could create a positive feedback loop where the spurs are continually supplied with nutrient rich water allowing their coral architects to develop more efficient channels for sediment movement. In this way, SaG morphology potentially exerts an important control over the sediment budget of carbonate platforms. Such insight is crucial for further understanding the role that SaG plays in the creation and stability of reef-top islands since their formation is largely determined by platform-margin hydrodynamics and the efficiency that sediment is exported from margin onto the platform-top (e.g. Kench et al. 2006; Smithers and Hopley, 2011; Mandilier 2012; Ruiz et al. 2013).

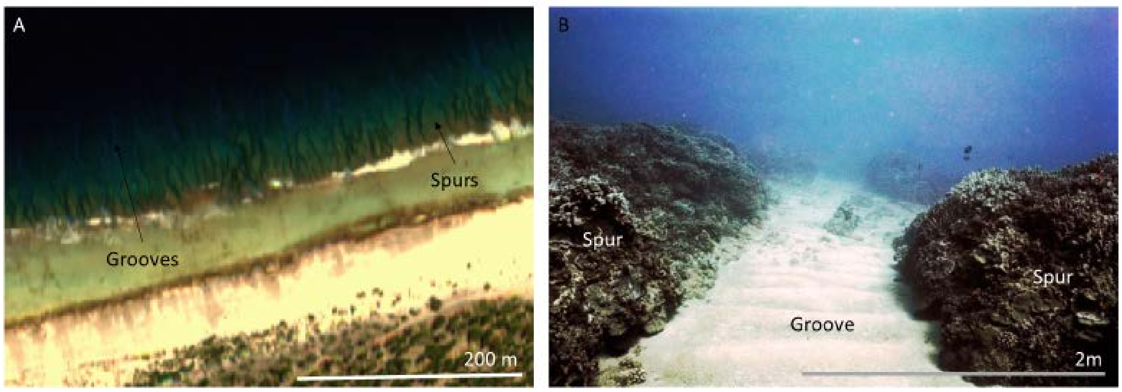


Figure 2. Two views of spur and groove morphology. Left is World View 2 satellite imagery of SaG from Tenarunga at two meter resolution; Right is taken from Rogers, et al., 2013. Spurs and a groove in Molokai, HI.

## 1.3 Controls on the development of spur and groove morphology

### 1.3.1 Wind and Waves as a Control on SaG Morphology Development

Shinn (1981) pitched the repeating pattern of SaG width to be controlled by the strength of the prevailing waves, with the definition of the grooves increasing with increasing wave energy. In the same vein, Roberts (1974) noted SaG morphology to vary according to the direction of the run-up of swell on the platform-margin. Munk and Sargent (1954) aimed to explain the spacing of successive spurs as measured parallel to the axis of the reef margin. This “spur wavelength” was found to have a correlation to the directional distribution of wave power although no link was ever established that directly connected specific thresholds of wave power to specific SaG spacing patterns. More recently, Kan et al. (1996) examined how the SaG morphology was orientated to the reef margin and suggested that the orientation of SaG is orthogonal to the direction of incoming waves. Roberts (1974) also noted that the spur amplitude, the vertical relief between the bottom of the groove and the top of spur, can be linked to the surrounding hydrodynamic regimes. This SaG amplitude mentioned by Roberts (1974), termed "regularity", refers to the consistent pattern of similarly sized (length- and width- wise) spurs separated by similarly spaced grooves. Examining the wind direction and wave energy of sites that do not exhibit this "regularity" after careful cross examination of SaG patterns and surrounding oceanographic conditions, could aid in explaining the importance of other factors such as platform shape as a control of SaG development.

### 1.3.2 Influence of Platform Shape on SaG and Carbonate Sediment Deposits

The interest in SaG morphology goes beyond just understanding its response to local oceanographic conditions. Positioned on the platform margin at the interface of fully developed marine conditions that lie seaward of the margin and the more sheltered platform-top environment, it can be assumed that understanding SaG morphology, and its variations, is important in the endeavor to reconcile the heterogeneity of Holocene platform-tops. Platform shape is relevant both to the development of SaG morphology and the formation of carbonate islands and cays because it dictates the degree to which ocean swell will be refracted upon contact with the platform and where wave energy will be focused (e.g. McIntyre et al., 1987; Kench 1988; Mendleier and Kench 2012; Ford and Kench 2013). While the SaG morphology acts as the physical conduit in which the sediment is transported, the platform shape plays a role in determining where on the platform a cay or island might develop (Gourlay 1988, 2011). Due to refraction, incoming wave energy will have varying effects on the SaG given the platform shape (Mandelier and Kench, 2012).

I hypothesize that the platform shape influences the degree to which SaG develop and organize themselves around the platform, which in turn carries over to influence the development and placement of carbonate deposits on the platform-top. This claim will be validated through my examination of a host of sites encompassing the three main variants of platform shape (circular, elongate, and angular) as put forward by Mendelier and

Kench (2012). Gourlay (1988, 2011) related platform shape and the establishment of cays to hydrodynamic focusing at a zone of energy convergence. A circular platform, for example, distributes wave energy along the margin move evenly than an elongate platform (Gourlay 1988; Mendlier 2014). In this vein, Gourlay (1988) believes that carbonate sediment islands found on circular platforms will shift and reform more than those on elongate ones. This difference arises because small differences in the angle of wave-approach will result in large changes in the area at which waves from opposing directions converge. However, in order for these convergence zones to produce platform-top cays, there must be a consistent supply of carbonate sediment. Ruiz et al. (2013) investigated the role that coral reefs play on sediment transport and found that the greatest amount of sediment transport occurred where the most skeletal debris is produced: along the shoreline where the reef-crest was shallowest and closest to shore. Given favorable hydrodynamics, this could create a positive feedback loop where the SaG is continually generating a supply of carbonate debris which in turn could be transported through the grooves and onto the platform-top. Investigation continues into the relationship found between varying platform shapes, the degree of development of SaG morphology that surrounds them, and the size and location of their respective sediment deposits. In this study, I suggest that sedimentation located behind stretches of well-developed SaG should remain static over time and further accumulate into more long lasting, stable deposits.

### 1.3.3 Sea Level Control on SaG Development

A rise in sea level serves to create accommodation space into which the spurs will aggrade with the result of accentuating the relief of the SaG morphology. By the same token, a sea level fall would serve to halt vertical aggradation of the spurs and instead promote lateral progradation (Gischler 2010). As such, while sea-level oscillation does not explicitly sculpt the morphology, it can serve to modify its architecture. This hypothesis is logical considering the weight of evidence showing sea-level fluctuation to be an important control of reef development in general (e.g. Camoin et al., 1997; Flemming et al., 1998; Andrefouet et al., 2009; Hongo & Kayanne, 2010; etc.). Fortuitously, the Holocene sea level curve is well constrained in the Pacific and Indian Oceans, the locations of my study sites, and therefore morphological outliers that I identify, such as tiered SaG morphology extending far seaward beneath the surf zone and hence likely built at a time of lowered sea level, can be related to the Holocene transgression.

# 2 Methods

## 2.1 Site Selection

To investigate SaG morphology around atolls that developed independently from one another and were shaped under differing oceanographic conditions, sites needed to be selected from around the globe, spanning multiple oceanic basins (Figures 1 and 3). Having sites of various size and shape also added to the list of variables that could be considered while analyzing the physical parameters that influence SaG morphology.

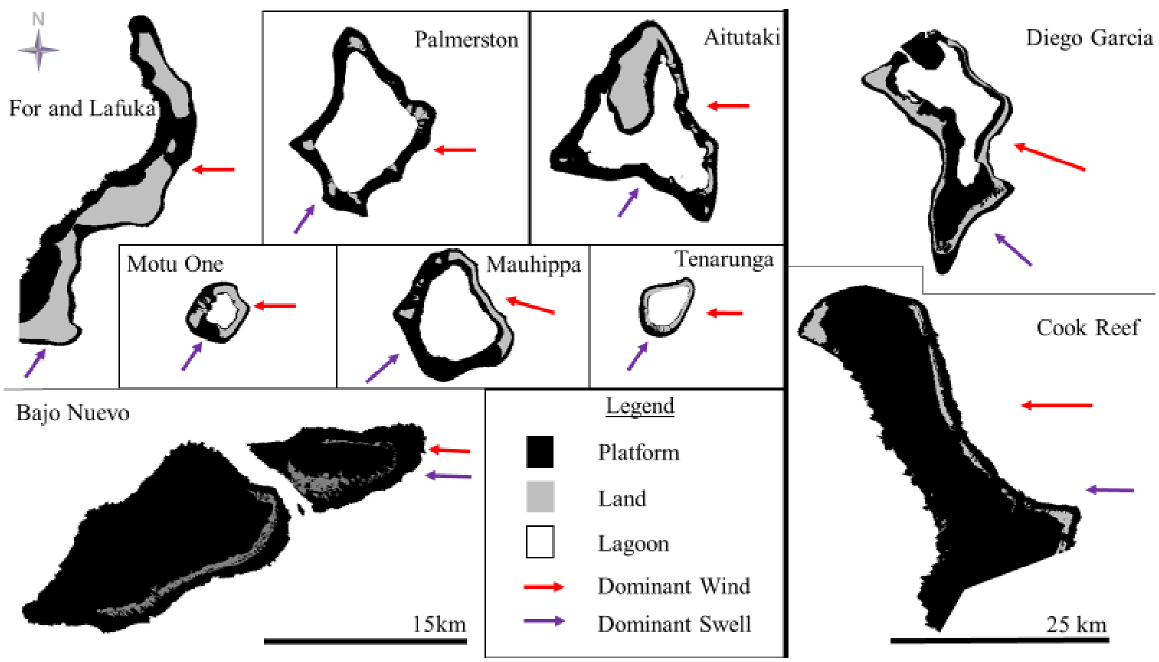


Figure 3. Visual representation of each of the nine sites and the prevailing wind and swell direction. The platform of the atoll is colored black with subaerially exposed cays and land colored grey.

### 2.1.1 Cook Reef

The site chosen from New Caledonia sits approximately 55 km Northeast of Ile Pott, the northernmost island of New Caledonia, at 18° 58’ S 163°34’ E. This site is a 35 kilometer long eastern flank of the barrier reef that circumnavigates New Caledonia. SaG on Cook Reef is most well developed and present on the eastern margin on this reef chain. The average wind speed for the year is 19 km/h. There is no seasonal preference for the direction the currents flow. However, the strongest currents which are on the order of 8 cm/s, tend to occur toward the middle section of the 35 kilometer elongate barrier reef under investigation in this study.

### 2.1.2 Foa and Lafka Islands

Foa and Lafuka Islands are two distinct islands sharing a carbonate reef platform and fringing reef in the Happai region of Tonga at 19°45' S, 174°19' W. The SaG analyzed from this site is present on the 26 kilometer stretch of fringing reef. The average wind speed from the southeast is around 17 km/h. SaG is present and well developed on the protruding areas of the margin which lends itself to more exposure to the wind and wave energy shaping the morphology. While wind and swell do not change course seasonally, this site does see seasonal changes in currents which exhibit a southward flow in the summer and a northward flow in the fall and winter time at an average of 10 cm/s.

### 2.1.3 Palmerston

Palmerston Island sits isolated in the South Pacific as part of the Cook Islands at 18° 02'S, 163° 09' W. Palmerston receives a year-round battering of winds from the east to east southeast. However, the same story cannot be said for the ocean swell impacting the atoll. In the summer months, Palmerston receives swell predominately from the south southwest. In the winter, swell is scattered in its approach and recorded from the north northwest, south southwest, and a minor percentage continuing to approach from the east. SaG development is stronger on the southern facing stretches of reef margin while the northern regions exhibit poorly developed SaG. The currents surrounding Palmerston approach from the east and southeast with virtually no seasonal variation at an average velocity of 15 cm/s.

### 2.1.4 Aitutaki

The atoll of Aitutaki lies at 18° 52' S, 159° 47' W and is part of the larger Cook Island chain in the South Pacific Ocean. Located within the trade wind belt, winds blow at a mean velocity of 13 km/h from the east to southeast and dominate in the winter months (Rankey et al, 2009). These winds produce waves from the same direction although the majority of Aitutaki's wave climate comes from southwesterly swell. Aitutaki's shape favors no area more so than another in terms of SaG development the atoll. The tidal currents show no discernable pattern of velocity or directionality between winter and summer months and remain below 15 cm/s.

### 2.1.5 Motu One

Motu One is located at 15° 49' S, 154° 31' W. Motu One receives winds blowing mostly from the east with slight derivations to the northeast and southeast. Swell approaches the atoll from the south southwest for the majority of the year with minor variations coming in the winter months when some swell registers from the west. Due to the small size of Motu One, wind and wave energy seem to be able shape moderate to well-developed SaG nearly all around the island. There was no seasonal preference for the direction which the currents moved over the platform at an average speed of 6 cm/s.

### 2.1.6 Mauhipaa

Mauhipaa is an atoll located in the Western extent of French Polynesia at 16° 48' S, 153° 57' W. The atoll is subject to winds from the east and east southeast for the duration of the year with no prolonged shift in directionality. The swell approaching the atoll arrives from the south southwest during the summer months but develops an additional westerly trend in the winter months. SaG at Mauhipaa is best developed on the southern and northern margins with the western margin showing moderately developed SaG, and the eastern margin exhibiting poorly developed SaG. The ocean currents surrounding Mauhipaa show no trends or preference in seasonal directionality. However, one aspect of the currents which remains a constant is their average speed of around 7 cm/s.

### 2.1.7 Tenarunga

Tenarunga sits in the far eastern edge of French Polynesia at 21° 20' S, 136° 32' W. Wind comes in predominantly from the eastern direction in the winter months and slightly from the southeastern direction in the summer months with an average speed of

25 km/h.  The SaG at Tenarunga consists of all moderate to well developed morphology most likely due to the circular shape of the atoll, ideal for dispersing incoming wind and wave energy uniformly.  The swell data show year round swell approaching Tenarunga from the southwest and south southwest.  Current directionality and speed did not show any pattern or preference for season.

### 2.1.8 Bajo Nuevo

Bajo Nuevo Bank is located nearly in the middle of the Caribbean Sea at 15° 50’ N, 78° 39’ W.  Bajo Nuevo is almost entirely submerged with only a few low laying cays along its southern flank breaching the surface of the water.   The bank is exposed to winds that come mainly from the east at 22 km/h with nearly no seasonal variation. Swell arrives on this eastern margin of Bajo Nuevo year round as well. SaG on Bajo Nuevo is best developed on the curved corners of the platform margin and the degree of SaG development declines rapidly as the fore reef slope makes its way towards the leeward margin.  The currents also do not exhibit any seasonal changes and, like the wind and the waves, arrive from the east and are typically around 20 cm/s.

### 2.1.9 Diego Garcia

Diego Garcia is an atoll situated in the British Indian Ocean Territory at 7° 18’ S, 72°26’ E.  Located in the intertropical convergence belt, the atoll receives the southeasterly trade winds during the summer months and then northwesterly wind in some of the winter months with a yearly average of around 16 km/h.  The same seasonal change in direction can also be applied to incoming waves, although waves from the south southeast are predominant in the summer. SaG at Diego Garcia is highly developed along the western, eastern, and southern regions of the atoll with the promontories in all regions exhibiting well developed SaG.  The tidal currents showed some correlation to the changing season with wintertime currents heading to the north and slightly northwest and summertime currents reversing that trend.  During both seasons, the stronger currents reach between 15 to 20 cm/s.

## 2.2 Site Imagery

Site selection was based primary on the availability of high resolution World View 2 satellite imagery collected as part of the Khaled bin Sultan Living Oceans Foundation's Global Reef Expedition. The World View 2 satellite offers multi spectral imagery with a resolution of two meters per pixel. Although at first sites were restricted to only stops on the expedition which focused heavily on areas in the South Pacific, an effort was made to ensure that sites from various ocean basins were selected. In that same vein, sites with varying degrees of platform size and shape were also sought in order to increase the number of variables. Although Diego Garcia was not a stop on the Global Reef Expedition, World View 2 imagery was obtained and utilized from another geospatial project to keep spur and groove analysis consistent across all sites.

## 2.3 Ocean Climate Data

In order to establish predominant windward and leeward margin of the platform and to further investigate the roles currents, waves, and wind influence the development of spurs and grooves, oceanographic data needed to be assembled for the waters surrounding each study site. Ocean current data were collected from HYCOM, a hybrid, generalized coordinate ocean model (www.hycom.org) that captures current magnitude and direction at a resolution of 1/12°. HYCOM datasets consisting of mean current magnitude and direction, termed "u" and "v" vectors at monthly averages were compiled in a spreadsheet according to their respective latitude and longitude. Using the four variables of "u", "v", latitude, and longitude, a formula created in Excel extrapolated the incoming angle of the ocean surface currents at each site. These data were used to find if there were any seasonal trends in current direction for each site (Figure 4). Wind and swell roses were gathered from two online sources (www.wisuki.com; www.windfinder.com), that archive historical weather data from local airport and ocean buoys. For most sites, a weather station was located on the island or close to shore. For sites that lacked their own unique weather station, such as Tenarunga, wind and swell data would be taken from sites surrounding the island in order to extrapolate the most accurate representation of forces impacting the site. The wind and swell roses were then utilized to assess any seasonal trends which could be used in interpreting patterns in SaG morphology.

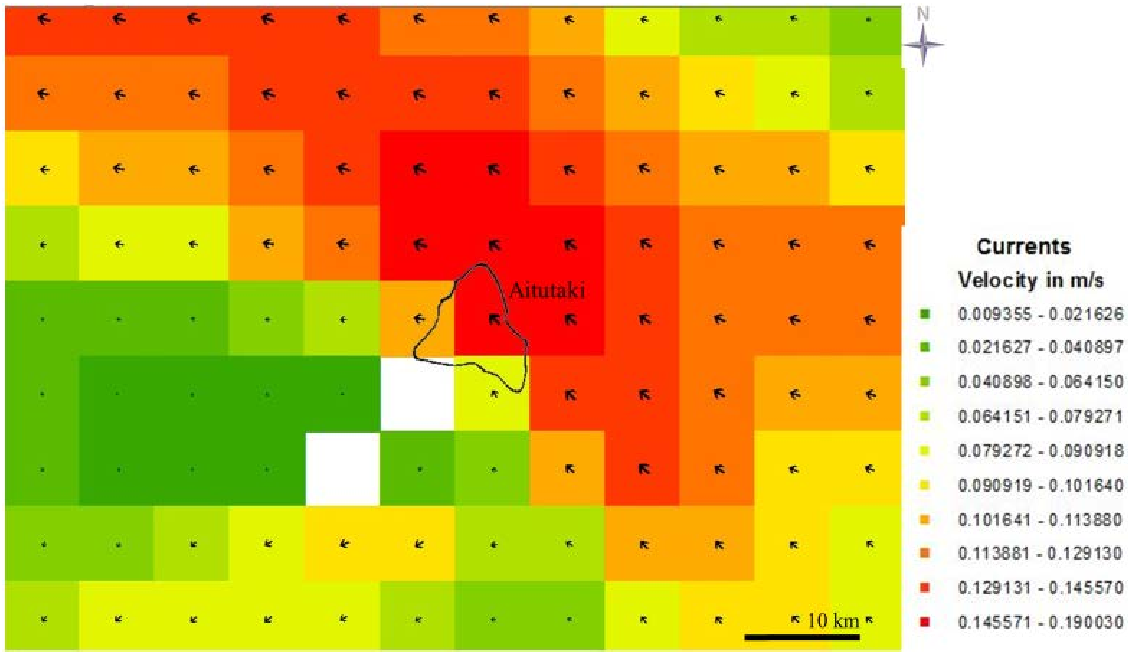


Figure 4. Example of a visual representation of current data from HYCOM. Shown here is one month's average velocity and direction around Aitutaki. White cells denote areas devoid of data.

## 2.4 Mapping the SaG Zone

The area of the carbonate platform containing the SaG morphology, the Fore Reef Slope (FRS) needed to be singled out on each site to focus further geomorphological analysis as well as observe the FRS differences between sites from a spatial regard. The upper region of the FRS, is defined by what is called the reef crest and is where the waves break over the reef. The lower region of the FRS extends seaward and terminates at the reef wall of the carbonate platform. Using Global Mapper software, a polygon was constructed which contains the SaG morphology starting at the reef crest and ending where the platform was too deep to detect via investigation of the satellite imagery (Figure 5A). This polygon was turned into a shape file and then read into a script created in Matlab which creates a "heat map" based off a virtual spine that runs through the middle of the polygon. The script takes into account the spatial resolution of a single pixel, two meters, and uses that information to color code the other pixels according to their perpendicular distance away from the centerline. Warmer colors represent a large distance between the centerline of the polygon and its periphery, whereas cooler colors are present where the centerline is relatively close to the polygons edges (Figure 5B). When the finalized heat ribbon is placed as a layer atop the satellite image, it offers a quick way to visualize where SaG morphology is prominent and well developed, that is, extending quite far seaward. With the basic constraints of the SaG morphology now delineated, areas of interest (i.e., areas sharing similar heat ribbon widths on opposite sides of the platform) can be readily marked for further investigation.

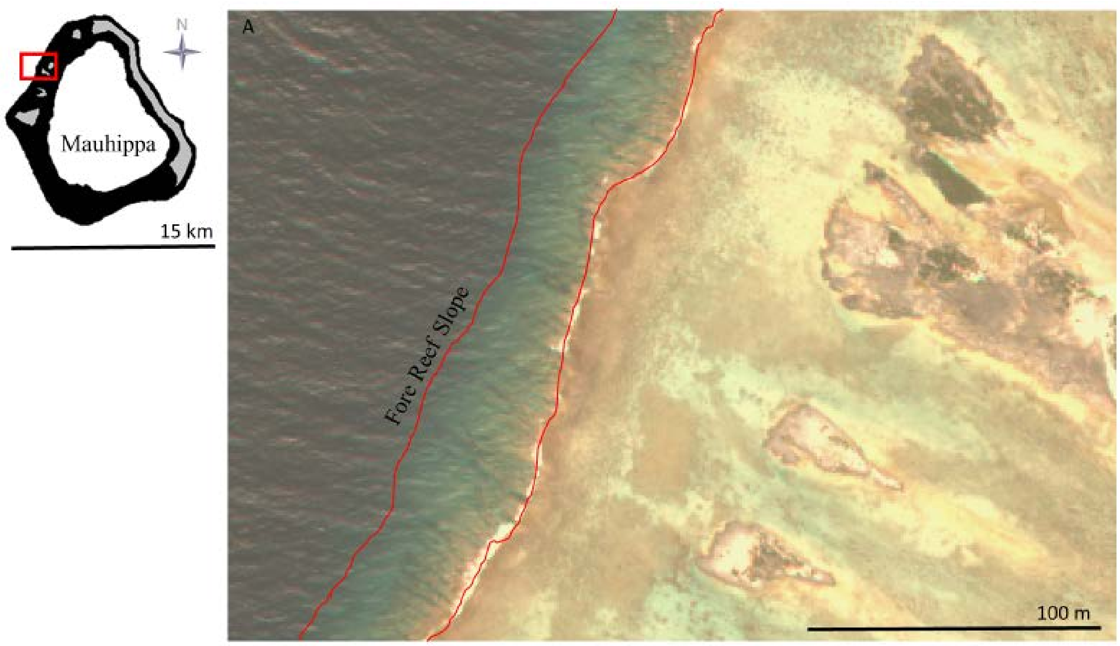


Figure 5. A) Red lines depict the seaward and reef crest-ward constraints of the Fore Reef Slope (FRS). The FRS begins where waves can be observed breaking over the reef crest and the FRS terminates where the slope blends into the surrounding sea. Mauhippa is used here as an example.

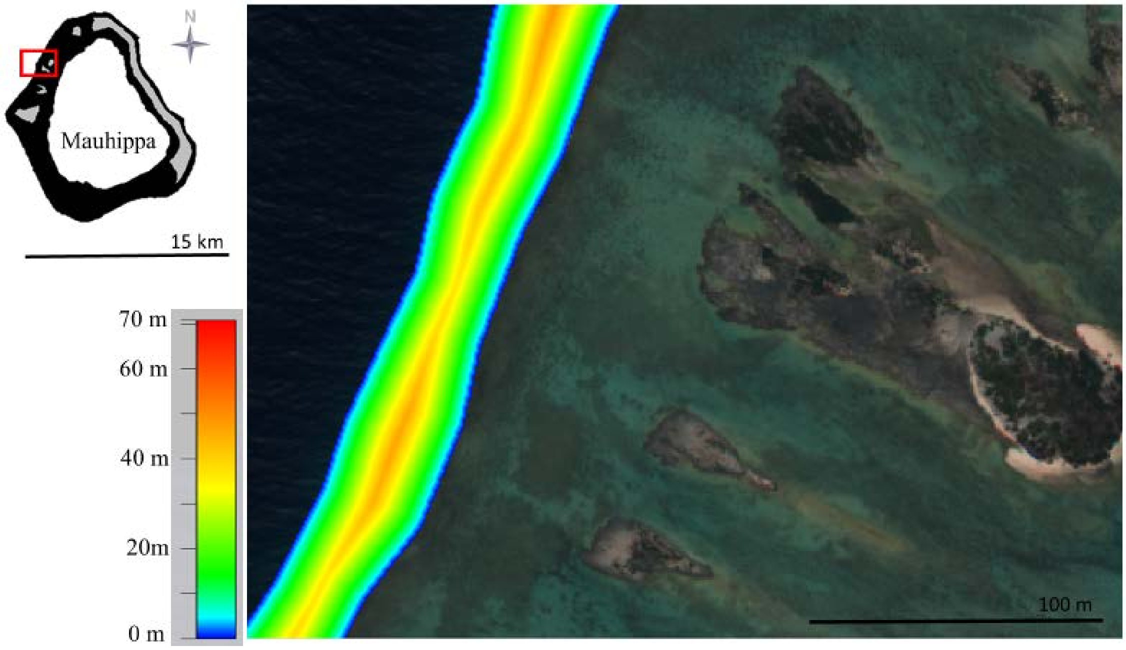


Figure 5. B) Heat map illustrating the width, in meters, of the FRS shown in Figure 5A. FRS width is calculated by multiplying the value of the colored pixel within the heat map by two.

## 2.5 Mapping the SaG Morphology

In order to make the SaG morphology more versatile in its ability to be used in spatial analysis procedures, digitization of the grooves needed to be done. As Figure 6 shows, grooves could be identified as the dark channels running perpendicular to the reef crest. Using a measurement tool within Global Mapper, the width of the groove was measured and then rounded to the nearest half meter. A line was then drawn down the center axis of the groove and assigned its measured width as an attribute. For each of the nine study sites, grooves were measured around the entire platform until all visible and unobstructed grooves were accounted for. All digitized grooves were then exported as a .tiff file with a sample resolution of a half of a meter to ensure the sharpest distinctions could be made in later steps of the digital groove analysis.

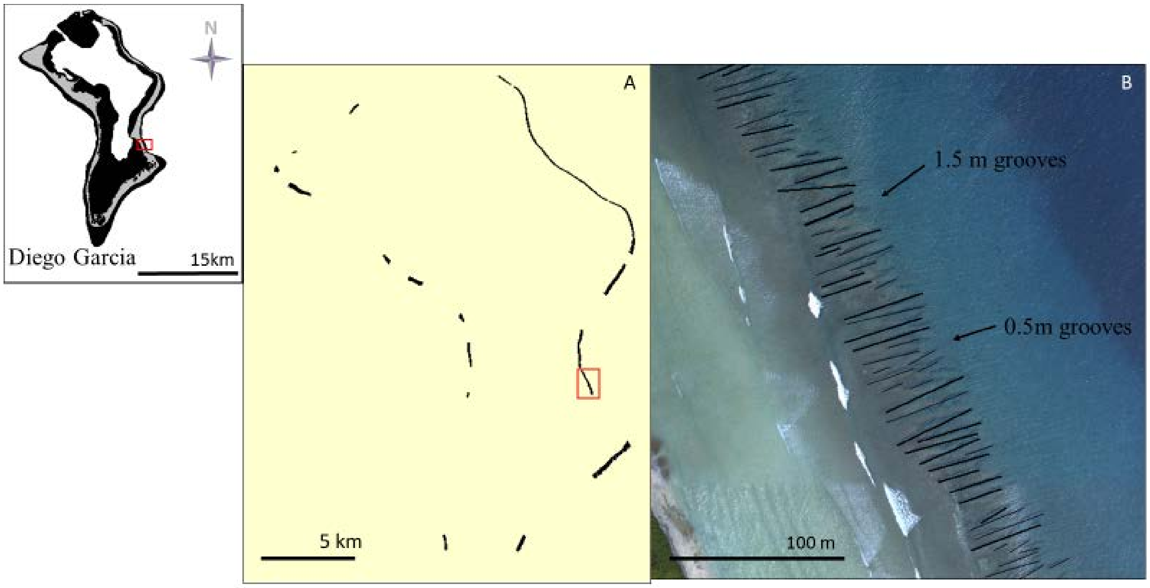


Figure 6. Digitization of the grooves around Diego Garcia. A) All observable grooves were digitized around each site. Areas missing digitized grooves either were devoid of any SaG morphology or the satellite imagery was compromised. B) A closer look at the digitized grooves with width attributed to each groove.

## 2.6 Analysis of the SaG Morphology

### 2.6.1 Fast Fourier Transform (FFT) Analysis

For comparing and contrasting the spatial periodicity, or the spacing of the grooves around the platform, a mathematical approach that could identify intrinsic spatial patterns was needed to explore possible controls both within and between various study sites. Fast Fourier Transform (FFT) is an algorithm designed to quickly perform a power spectrum analysis of a time series (Cochran et al., 1967). Essentially, the algorithm is designed to look at the frequencies of a signal compromised by noise and neatly present to the user the inherent dominate frequency, secondary frequency, and so on (Figure 7A). For this study, FFT was used to explore the spatial periodicity of SaG along strike around each of the study sites. The graph of the output in an FFT equation has a designated power spectrum representing the Y-axis and range in frequency being shown along the X-axis. Although the FFT is designed to work on an infinite signal over a temporal scale, for this study I have altered it to suit the needs of my investigation by working on a finite signal over a spatial scale. Inspiration to carefully change the algorithm's intended application comes from the study done by Harris et al. (2010), in which they investigated the spatial parameters of carbonate sand deposits on Grand Bahama Bank. The Matlab script which implements the FFT first calls for two inputs: a "Geo Tiff" file of the digitized grooves under investigation and a shape file of the transect line running over that aforementioned section of SaG. Next, a binary barcode is generated from the points of intersection where the transect passes through the digitized grooves. This simple binary image has grooves represented by a "zero" and spurs represented by a "one" (Figure 7). This string of zeroes and ones is then used as the input "x" for Matlab's FFT function "Y = fft (x)." The FFT function analyzes the barcode as if it were a continuous signal, like a section of a sine wave, and then outputs the inherent width patterns in the bar code signal. It is important to note that the value of the primary frequency acts only as an aid in deciphering the dominant spatial pattern inherent in the SaG being investigated by the FFT. Referral back to the satellite imagery was needed to properly interpret what the graph is showing: the most commonly occurring groove width. The FFT was run on SaG from each site and for each SaG ranking if the ranking was present to compare and contrast the resulting primary and secondary signatures. Areas to be analyzed were selected based on if the expanse of SaG was in an area of the satellite imagery that lent itself to unobscured analysis.

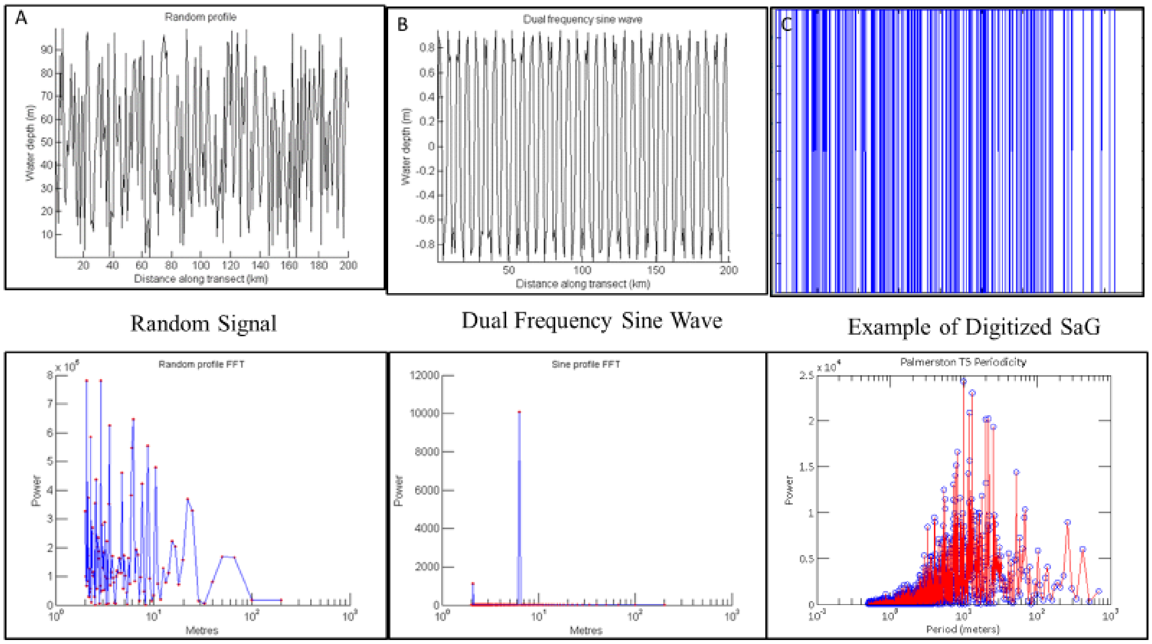


Figure 7. Different examples of FFT results. A) FFT picking out various frequencies of a random signal. B) A dual frequency sine wave will clearly show a primary and secondary peak. C) An example of what digitized grooves look like when turned into a signal and how FFT attempts to pick out intrinsic frequencies.

### 2.6.2 Visual Ranking of SaG Development

A major aspect of this study was ranking the SaG morphology on a scale from 1 through 5 as a means to assess the SaG level of development and organization. Within ArcGIS, a line was drawn around a satellite image of the site and then that line was divided into 100 meter segments (Figure 8). The visible SaG contained in each segment was then closely inspected and assigned a ranking based on the criteria listed in Table 1, Figure 9.

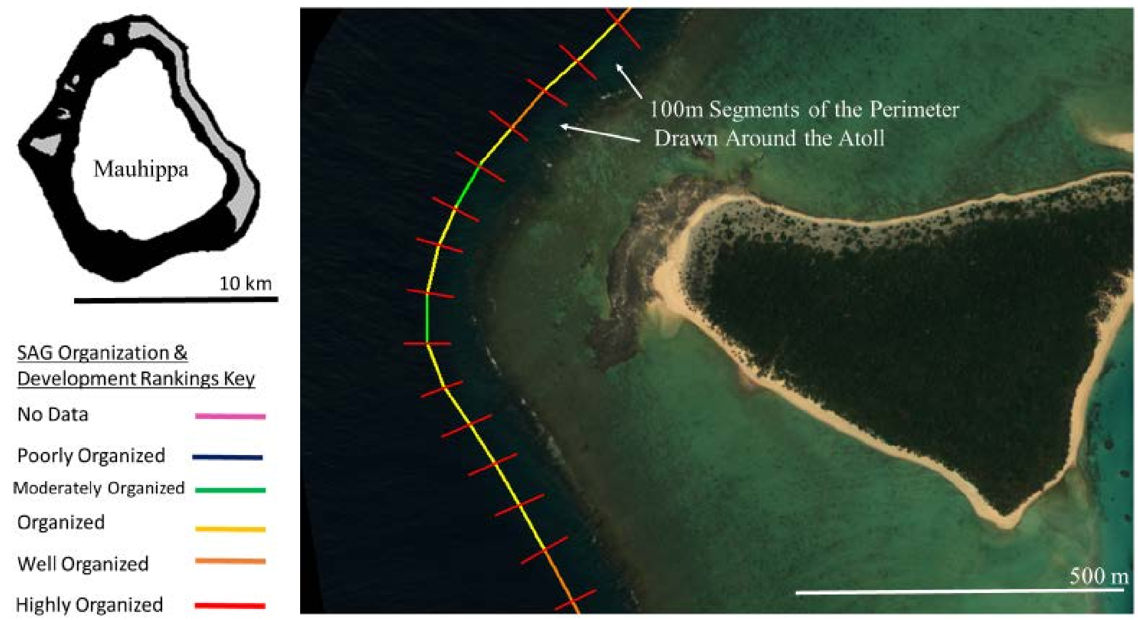


Figure 8. Figure showing the perimeter drawn around Mauhippa divided into 100 meter sections. The degree of organization and development of the SaG within these sections determined the color of the sections.

Table 1. Criteria Used in Ranking Spur and Groove Organization and Development

| Ranking And Name | Criteria | Demonstration |
|---|---|---|
| **0**<br>SaG<br>Absent | Spur and Groove Morphology Absent | Figure 9A |
| **1**<br><br>Poorly Organized SaG | Grooves do not create a continuous channel from the reef crest to the seaward termination of the SaG Zone<br>Grooves may express themselves perpendicular to the reef crest<br>Throughout 100m audit section, a spurs width will vary greatly from its neighboring spur<br>Spurs can be orders of magnitude wider than their surrounding grooves<br>Groove width, on average, starts off wider near the reef crest and narrows as it extends toward the seaward termination of the SaG Zone | Figure 9B |

| | | |
|---|---|---|
| **2**<br><br>Moderately Organized SaG | Spurs are not a single, continuous feature from reef crest to seaward termination<br>Spurs are highly multi-directionally bifurcated creating a maze-like collection of groove from reef crest to fore reef slope<br>Spurs length can vary anywhere between 5m to 75m | Figure 9C |
| **3**<br><br>Organized SaG | Spur width, and groove width, become more consistent within the 100m ranking audit section.<br>Spur bifurcation runs parallel to the “parent” spur’s axis<br>Spurs are, on average, wider than their adjacent grooves<br>Spurs may also regroup into a solid unit of reefal material towards the edge of the reef platform. | Figure 9D |
| **4**<br><br>Well Organized SaG | SaG exhibits only minor variations in spur and groove width throughout the 100m audit section<br>The spurs, as well as the grooves, maintain their measured width for >50% of their seaward extension<br>Detached spurs may be present but still maintain the average width of neighboring spurs within audit section | Figure 9E |
| **5**<br><br>Highly Organized SaG | SaG exhibits consistent spur and groove width for the duration of the 100m audit sections<br>Spur width is nearly constant from spur formation to seaward termination.<br>Spur length extends seaward for hundreds of meters from the reef crest.<br>SaG meander and bifurcation is absent. | Figure 9F |

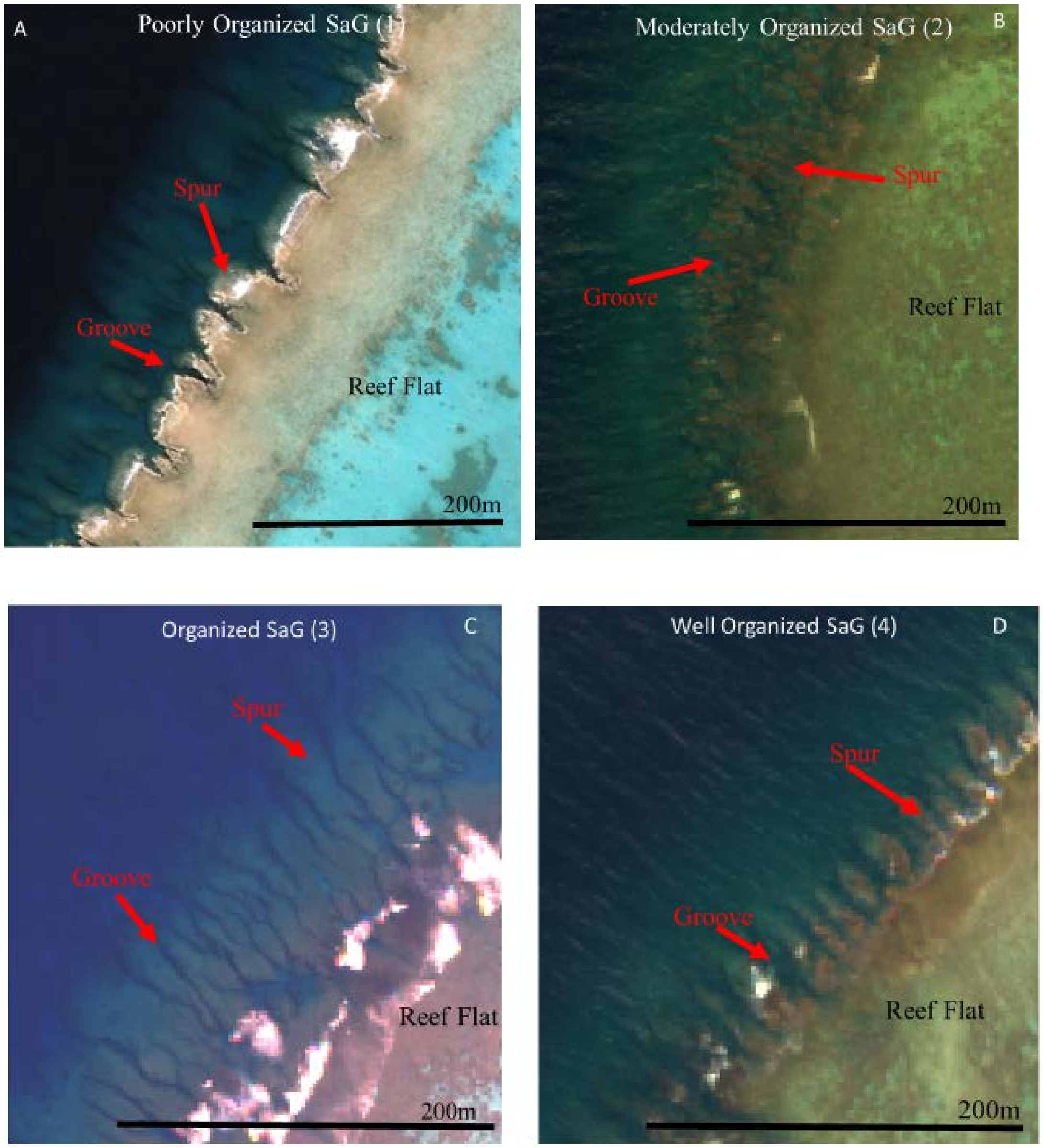
A
Poorly Organized SaG (1)
Spur
Groove
Reef Flat
200m
Moderately Organized SaG (2)
B
Spur
Groove
Reef Flat
200m
Organized SaG (3)
C
Spur
Groove
Reef Flat
200m
Well Organized SaG (4)
D
Spur
Groove
Reef Flat
200m

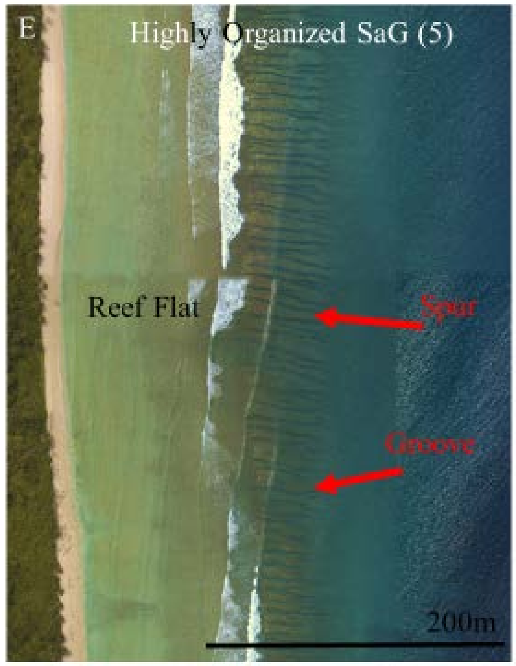


Figure 9. A-F Showing the various degrees of SaG organization and development as mentioned in Table 1. SaG development can be seen improving as SaG organization grows tighter.

### 2.6.3 Precinct Analysis

To better make use of the SaG ranking data, six areas of the FRS at each site were isolated to offer a closer examination of the SaG development and how it varied around the platform. These isolated areas, termed precincts, were situated on the curved promontories as well as the straighter expanses of the SaG zone with each windward precinct assigned a leeward counterpart and each swellward precinct assigned a complementary swell-protected precinct. An effort was made to make sure each precinct also matched its counterpart in length as closely as possible to maintain a level of consistency (Figure 10). By comparing precincts on opposite margins of the atoll, this allowed for analysis on the influence of SaG location and margin shape on the overall development of SaG.

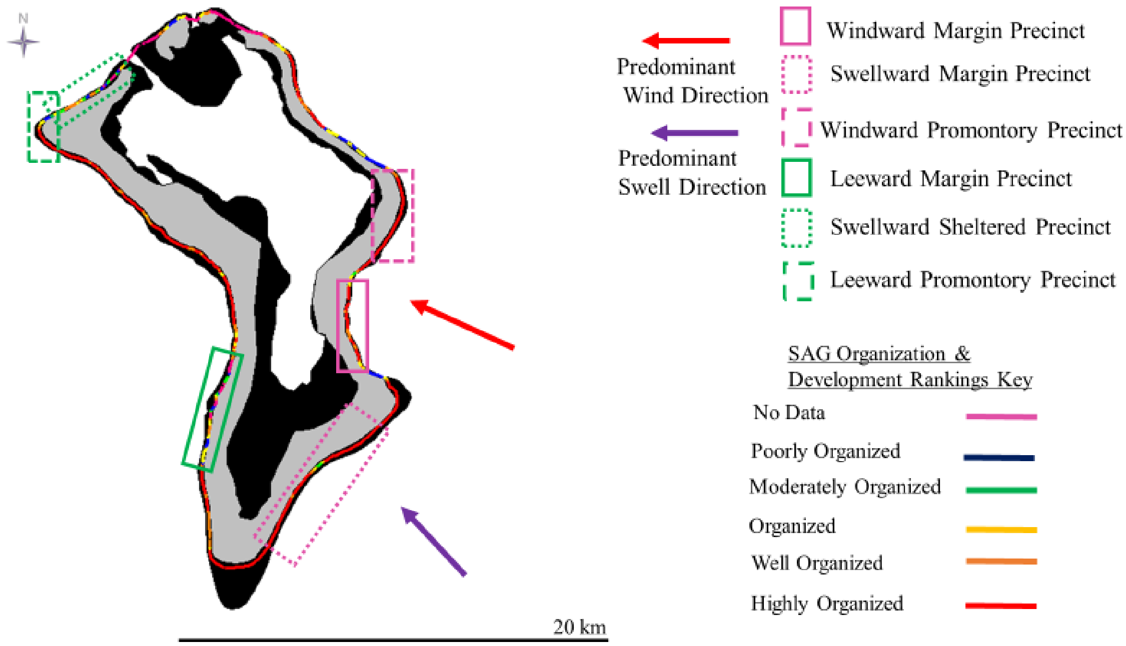


Figure 10. Diego Garcia being used as an example of precinct map used on all sites showing how precincts were determined based of dominant wind and swell direction as well as platform shape.

### 2.6.4 Binomial Testing

Using the ranking data contained within each precinct, further investigation into the proportion of highly-developed SaG (SaG receiving a rank of 4 and 5) was conducted in order to examine whether or not there is a significant difference in highly developed SaG between opposing precincts. Binomial testing was chosen as the strongest test of the null hypothesis that both the proportion of highly-developed SaG is equal between each individual pair of precincts. The test uses the binomial distribution of the precinct to decide if the outcome of an experiment using a binary variable can be attributed to a systematic effect. Written in R, the equation used calculated the proportion of highly developed SaG in both precincts with the null hypothesis being that those proportions are equal with a confidence of 95%. If the p-value, or the probability that the precinct contained highly developed SaG, was lower than the alpha value it was saying that the proportion of highly developed SaG in one precinct SaG would be statistically significant from the proportion of highly developed SaG in its opposing precinct and that difference is not by chance.

### 2.6.5 Reef Flat Zone Analysis

For investigation into how well developed SaG may act as a conduit for sediment transport onto the platform, it was important to take measurements of a back reef area adjacent to SaG. The area of the atoll that would be included in this measurement was termed “Reef Flat Zone” (RFZ). For this study, the RFZ was classified as comprising of the reef crest, the reef flat, and the back reef prior as delineated in Figure 11A, B. The RFZ was delineated in Global Mapper and its width investigated in relation to adjacent SaG ranking for each site. Similar to the process used to create the SaG zone heat map, a polygon of the RFZ was constructed in Global Mapper and then converted into a shape file. Wide areas of the RFZ were dominated by warmer colors and narrow regions were cooler colors. Using the color gradients of the heat map as a guide, a line was traced throughout the center of the polygon to create what was referred to as a “centerline”. Next, the GIS layer for the SaG rankings which was divided into 100 meter sections for ranking assessment, was imported into the GIS. The centerline of the RFZ was then divided to correspond to the adjacent 100 meter sections of the SaG Rankings (Figure 11C). For each divisional point of the centerline, the underlying width value of the RFZ was audited and recorded into an Excel spread sheet. Plotting the width values alongside the SaG rankings offered insight into any correlation between the development of SaG and RFZ width (Figure 12).

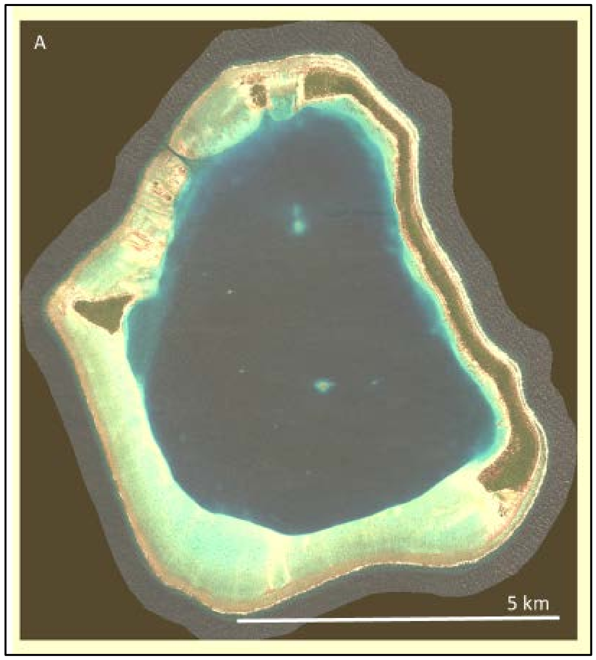
A
5 km

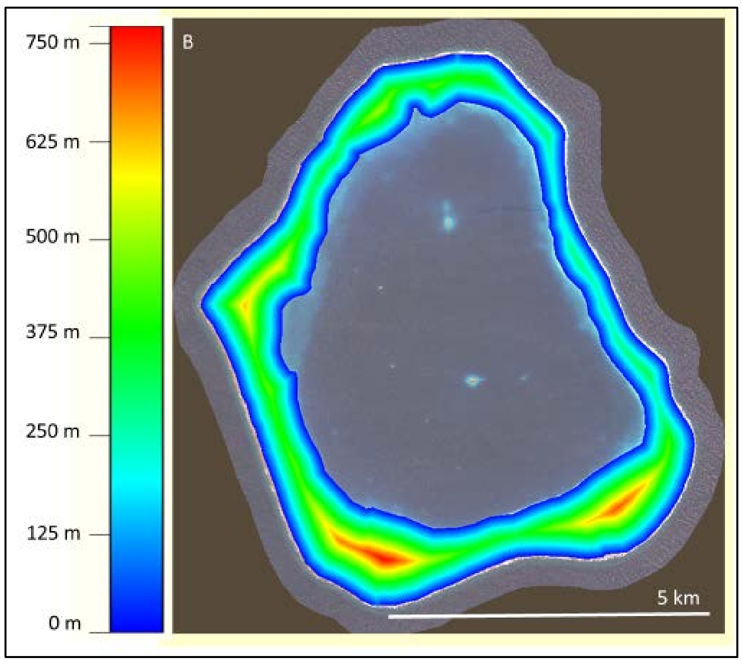
750 m
625 m
500 m
375 m
250 m
125 m
0 m
B
5 km

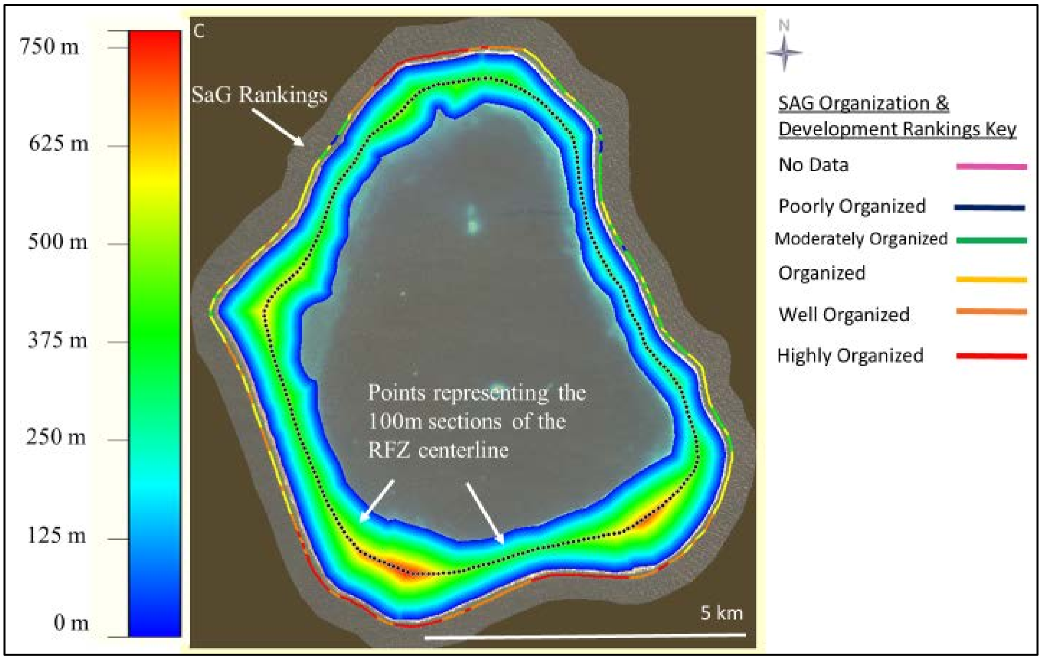


Figure 11. RFZ Identification. A) The Reef Flat Zone was chosen to comprise the reef crest, reef flat, and back reef. B) Once delineated, the polygon was run through a Matlab code to easily visualize and audit the RFZ width. C) A line run through the center of this heat map was then used to link up sections of the RFZ to its corresponding section of adjacent SaG located seaward.

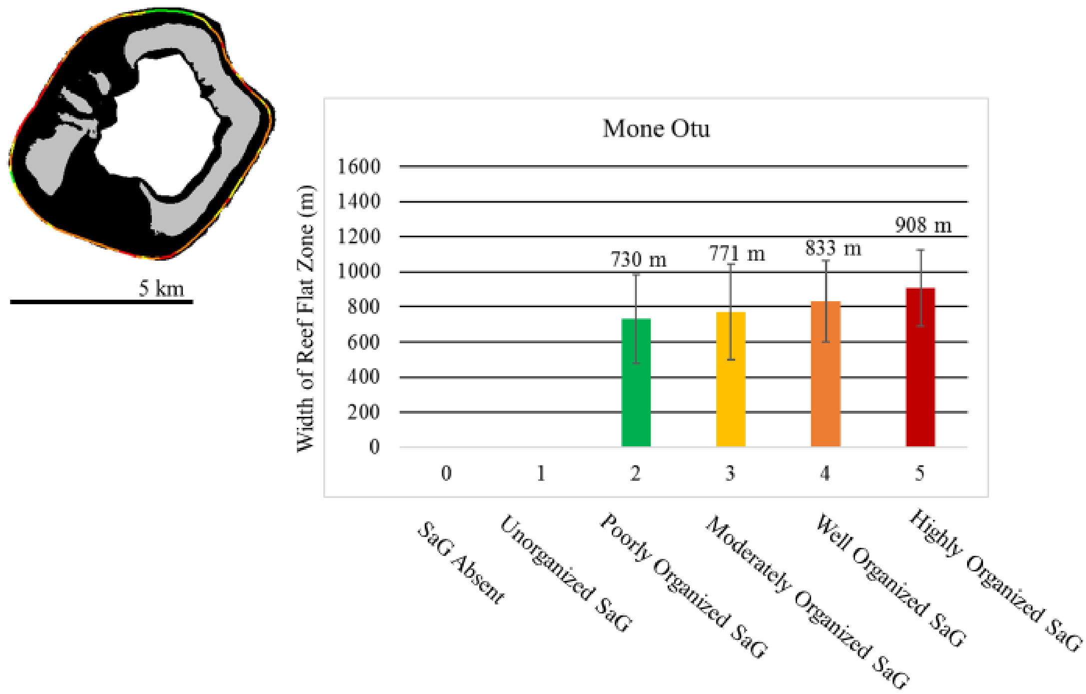


Figure 12. Graph showing the comparison between width of Reef Flat Zone (RFZ) and the SaG Ranking.

# 3. Results

## 3.1 Reef Flat Zone Width Analysis Results

### 3.1.1 An Overview of the Reef Flat Zone Relationship to SaG Morphology

The results of Reef Flat Zone (RFZ) analysis showed that the size and shape of the carbonate reef platform may have a role in determining the degree to which the SaG morphology influences the width of the RFZ. As Table 2 shows, the probability of there being a positive relationship between RFZ and SaG morphology was greatest for those sites that were the smallest in area and had curved, as opposed to angular, margins. As the sites moved into the medium to large range for this study (72 sq. km – 380 sq. km), the probability that there was no positive trend between RFZ width and adjacent SaG morphology increased. Three out of these five medium to large sites, Foa and Lafuka Islands, Aitutaki, and Cook Reef, expressed no clear linear trend between RFZ width and the degree of development of the SaG. Furthermore, in regards to platform shapes, the two sites with elongate platforms, Foa and Lafuka Islands, and Cook Reef, expressed no continuous linear trend in RFZ width increasing as SaG morphology improved.

Table 2. Platform size and shape listed along with the SaG rankings around each site and the related width of the adjacent RFZ. Blue cells indicate the RFZ width for the lowest SaG rank observed. Green cells indicate an increase in RFZ width from the previously ranked SaG. Red cells indicate a decrease in RFZ width from the previously ranked SaG.

| | | | Average Width (m) of RFZ Adjacent to SaG Ranked: | | | | | |
|---|---|---|---|---|---|---|---|---|
| **Site Name** | **Platform Size ($km^2$)** | **Platform Shape** | **0** | **1** | **2** | **3** | **4** | **5** |
| Tenarunga | 13 | Teardrop | N/A | N/A | N/A | 472 | 543 | 512 |
| Motu One | 16 | Circular | N/A | N/A | 730 | 771 | 833 | 908 |
| Mauhippa | 60 | Smoothed Diamond | N/A | 543 | 551 | 772 | 968 | 1021 |
| Palmerston | 64 | Diamond | 665 | 656 | 750 | 734 | 811 | 813 |
| Foa and Lafuka | 72 | Vertical Elongate | 1862 | 2975 | 3155 | 2255 | 2326 | 2319 |
| Aitutaki | 103 | Triangular | 839 | 1418 | 1628 | 1186 | 1227 | 919 |
| Diego Garcia | 190 | Double Tiered Diamond | 634 | 674 | 1018 | 804 | 1065 | 1157 |
| Bajo Nuevo | 205 | Horizontal Elongate | N/A | 417 | 361 | 450 | 1001 | 762 |
| Cook Reef | 380 | Vertical Elongate | 815 | 1048 | 1082 | 691 | 719 | 768 |

### 3.1.2 Cook Reef

As Figure 13 shows, Cook Reef is similar to Foa and Lafuka Islands in regards to an interrupted trend between average RFZ width and well-developed SaG. There is a positive trend for the first three rankings (0-2), a decrease in average RFZ width with for SaG ranked 3, and then the beginning of a positive trend again, albeit taking place within a different RFZ width range from rankings 3 through 5. Average RFZ width where there is no SaG present (n=59) is 814 meters. From there, average RFZ width increases to 1,048 meters when associated with SaG receiving a ranking of 1 (n=38). Again, an increase in average RFZ width by 53 meters to 1,081 meters is accounted for adjacent to SaG with a rank of 2 (n=19). However, SaG that received a rank of 3 (n=94), was found to be situated adjacent to the RFZ that averaged a width of only 691 meters, nearly 400 meters less than the RFZ where SaG received a rank of 2. For SaG with a ranking of 4 (n=151), the average RFZ width was 718 meters, an increase from the previous RFZ width and marked the beginning of the second positive trend for Cook Reef's SaG rankings versus average RFZ width. Lastly, SaG ranked 5 (n=87) corresponded to an average RFZ width of 767 meters.

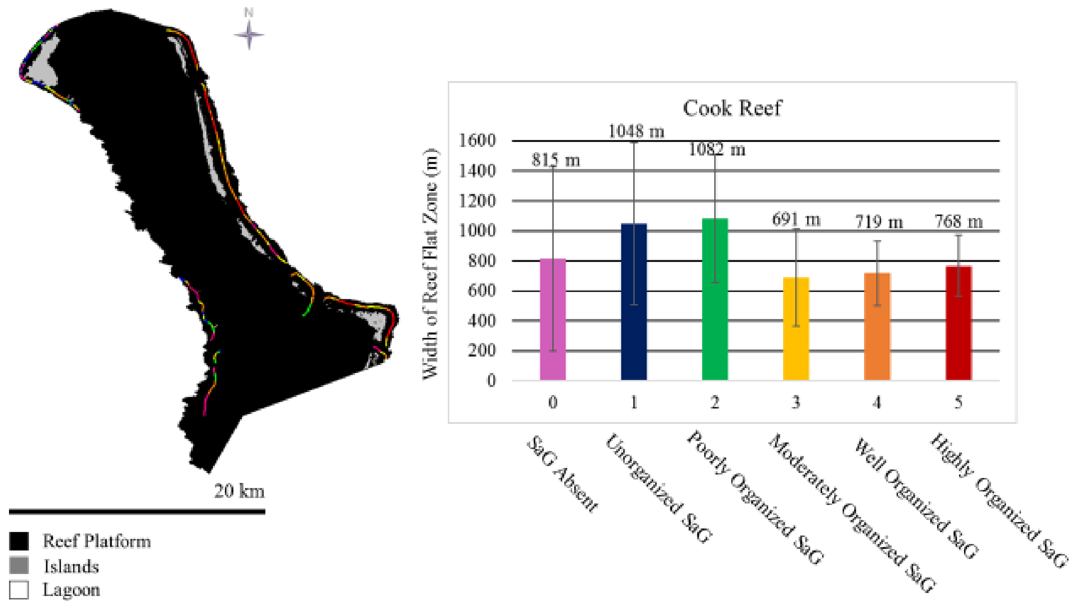


Figure 13. Showing relationship between RFZ width and SaG Rank for Cook Reef

### 3.1.3 Foa and Lafuka

Foa and Lafuka showed no consistent trend in regards to average RFZ width increasing as the SaG became more developed and organized.  Foa and Lafuka had an average RFZ width of 1862 meters where there were no SaG present (n=25).  Where SaG received a ranking of 1 (n=30), the corresponding average RFZ width increased to 2,975 meters.  In areas where SaG received a ranking of 2 (n=3), the corresponding average RFZ width again increased, this time to 3155 meters.  However, the average RFZ width decreased to 2255 meters when associated with SaG that received a ranking of 3 (n=84).  For SaG ranked 4 (n=112), the corresponding average RFZ width was 2326 meters, an increase from SaG ranked 3 but still a decrease from SaG ranked 1 and 2.  SaG that was ranked 5 (n=52) saw yet another decrease in its corresponding average RFZ width as it dropped to 2319 meters (Figure 14).

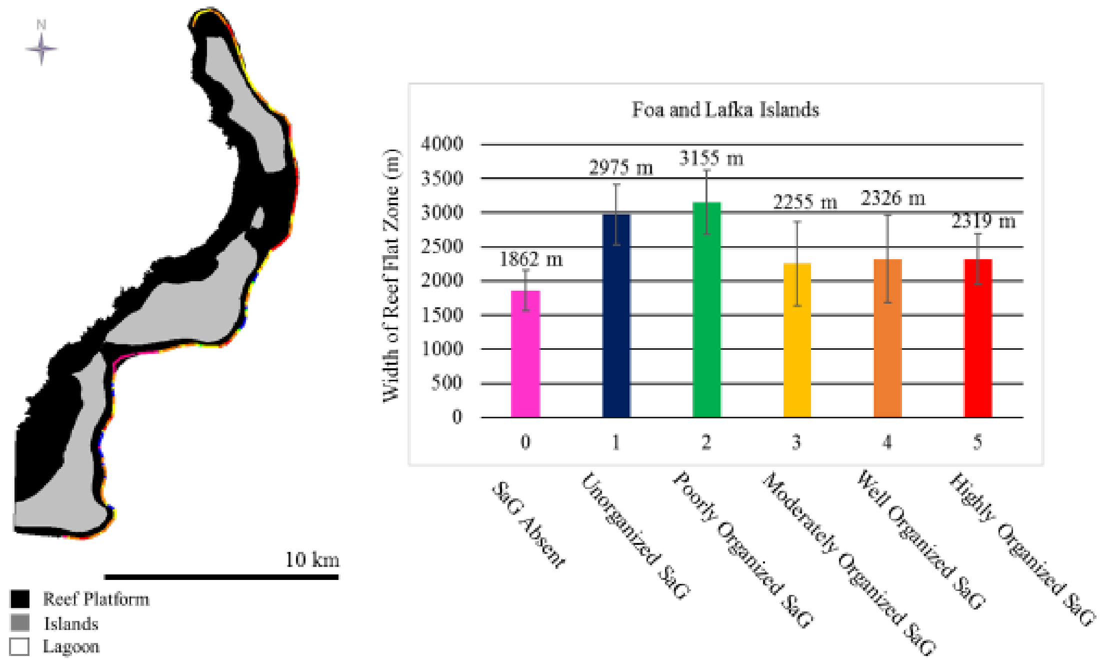


Figure 14. Graph showing relationship between RFZ width and SaG rank for Foa and Lafuka Islands.

### 3.1.4 Palmerston

While not a perfect linear trend of increasing average RFZ width corresponding with the incremental increase in SaG development, as Figure 15 shows, well developed SaG on Palmerston did coincide with a wider average RFZ when compared to the average RFZ width associated with less developed SaG. For areas where SaG was absent (n=4), the average RFZ width was 665 meters. Average RFZ width decreased slightly to 656 meters when situated adjacent to SaG that was ranked 1. There was then an increase in average RFZ width to 750 meters when associated with SaG ranked 2 (n=38). However, the average RFZ width decreased slightly to 734 meters where SaG was ranked 3 (n=147). For RFZ adjacent to SaG ranked 4 (n=72) the average width increased to 811 meters. Lastly, average RFZ width increased once more to 813 meters for areas of the RFZ that were associated with SaG that received a ranking of 5 (n=35).

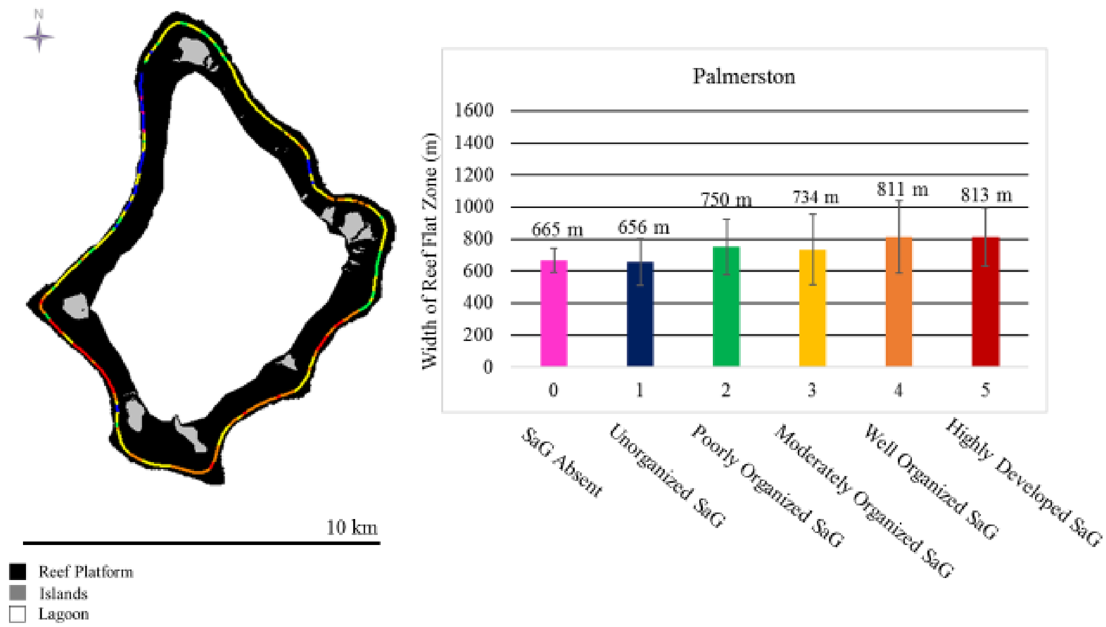


Figure 15. Graph showing relationship between RFZ width and SaG ranking for Palmerston.

### 3.1.5 Aitutaki

There was no consistent relationship between average RFZ width and the degree of development of SaG in Aitutaki as Figure 16 shows. While there was a positive trend noticed between average RFZ width and rankings 0 through 2, that trend absent for rankings 3-5. Furthermore, the average RFZ width for those areas associated with SaG ranked 3-5 did not even reach, let alone exceed, the widths of the RFZ associated with lesser developed SaG. For those areas of the RFZ where there was no SaG (n=23), the average width was 839 meters. Next, the average RFZ width where SaG was ranked 1 (n=131) was 1418 meters. Another increase in average RFZ width was observed for areas of the RFZ associated with SaG ranked 2 (n=37). Average RFZ width then decreased to 1186 meters where the adjacent SaG was ranked 3 (n=132). Average RFZ width then rose slightly to 1227 meters for those areas adjacent to SaG ranked 4 (n=100). Lastly, average RFZ width decreased by over 300 meters down to 919 meters for the area of the RFZ coinciding with SaG ranked 5 (n=16).

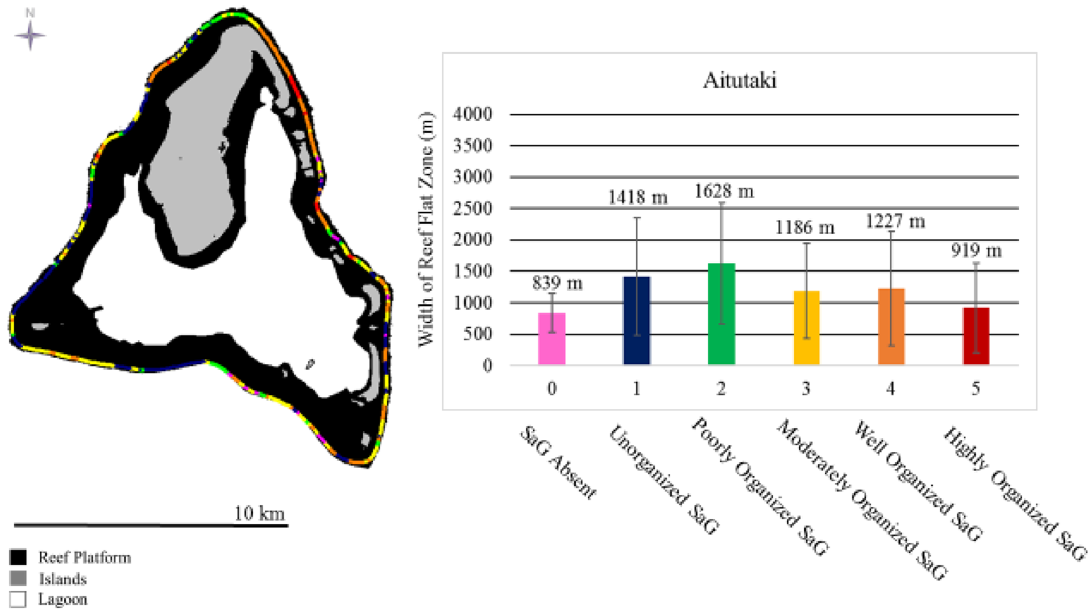


Figure 16. Graph showing relationship between RFZ width and SaG ranking for Aitutaki.

### 3.1.6 Motu One

Motu One, while lacking any SaG segments ranked with a 0 or 1, showed a clear linear trend of increasing RFZ width for SaG ranked 2 through 5 as displayed in Figure 17. SaG ranked with a 2 (n=11) corresponded to an average RFZ width of 730 meters. SaG ranked with a 3 (n=25) was found with an average RFZ width of 771 meters. In places where SaG earned a ranking of 4 (n=71), adjacent areas of the RFZ recorded an average width of 833 meters. Lastly, SaG with a ranking of 5 (n=25) was associated with an average RFZ width of 908 meters.

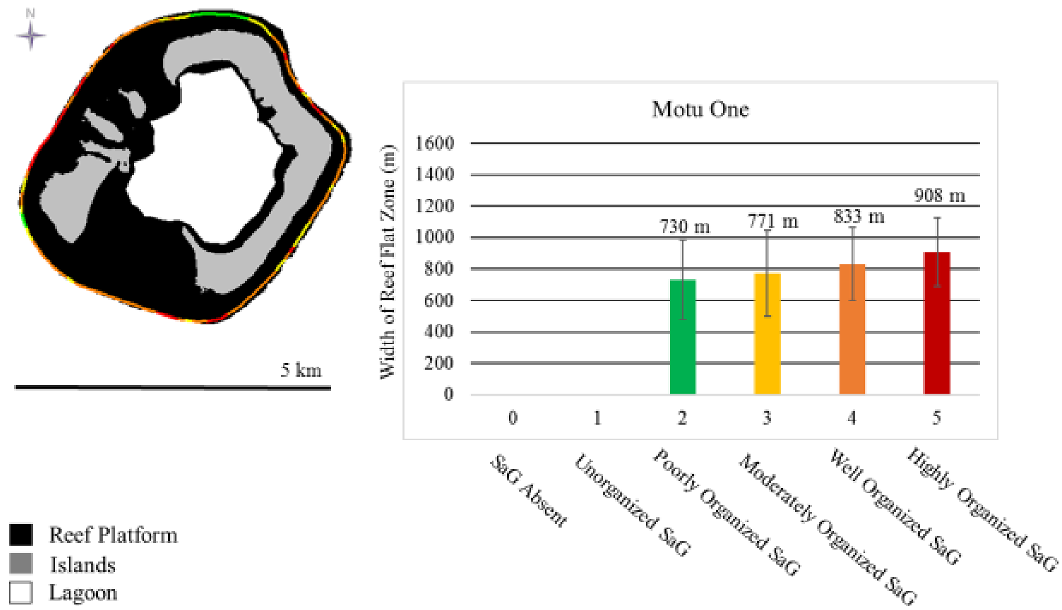


Figure 17. Graph showing relationship between RFZ width and SaG rankings for Motu One.

### 3.1.7 Mauhippa

Mauhippa showed a strong trend of increasing average width of the RFZ as the SaG rankings progressed from 1 through 5. There was no area along Mauhippa's margin that was absent from some degree of SaG development, therefore there are no rankings of 0. As Figure 18 shows, a SaG ranking of 1 (n=6) at Mauhippa was associated with an average RFZ width of 543 meters. A SaG ranking of 2 (n=49) was associated with a slight increase in average RFZ width to 551 meters. SaG ranked 3 (n=93) were tied to the largest increase in average RFZ width on Mauhippa resulting in an average width of 772 meters. Mauhipaa SaG with a ranking of 4 (n=72) were associated with an average RFZ width of 968 meters and SaG ranked 5 (n=61) were found adjacent to the RFZ where the average width was 1021 meters.

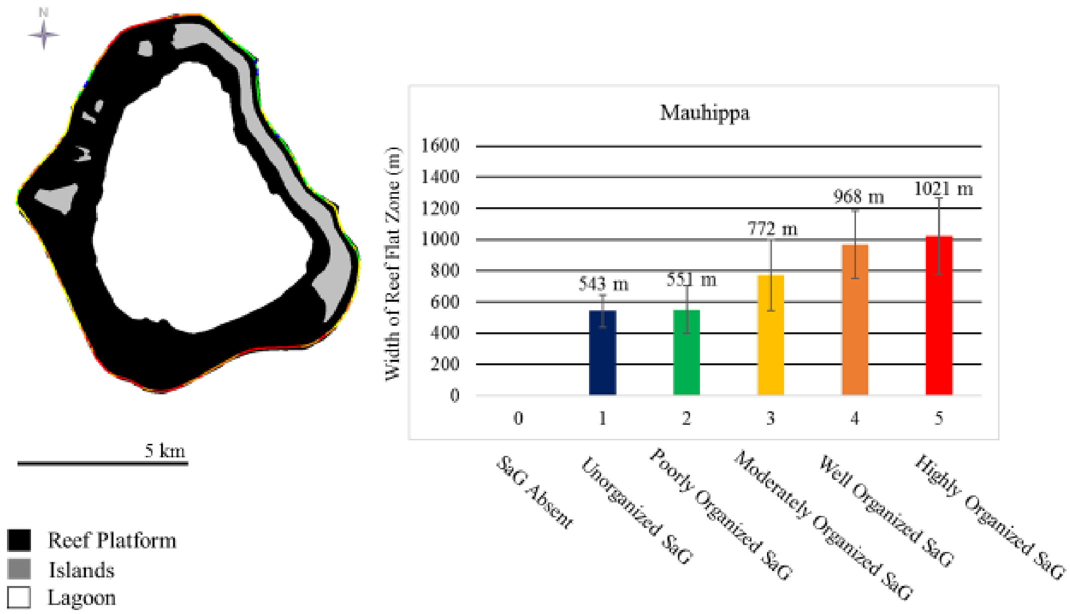


Figure 18. Graph showing relationship between RFZ width and SaG Ranking for Mauhippa.

### 3.1.8 Tenarunga

Tenarunga lacked SaG earning a rank of 0, 1, and 2. SaG ranked 3, 4, and 5, showed a slight trend of coinciding with an increase in the average width of the Reef Flat Zone (RFZ) as the SaG development and organization improved. As Figure 19 shows, the average width of the RFZ adjacent to SaG ranked 3 was 472 meters. The number of SaG segments, n, on Tenarunga that earned a rank of 3 was 18. The average RFZ width increased to 534 meters where SaG had a ranking of 4 (n=50) and then only slightly decreased to 512 meters where the SaG received a ranking of 5 (n=67).

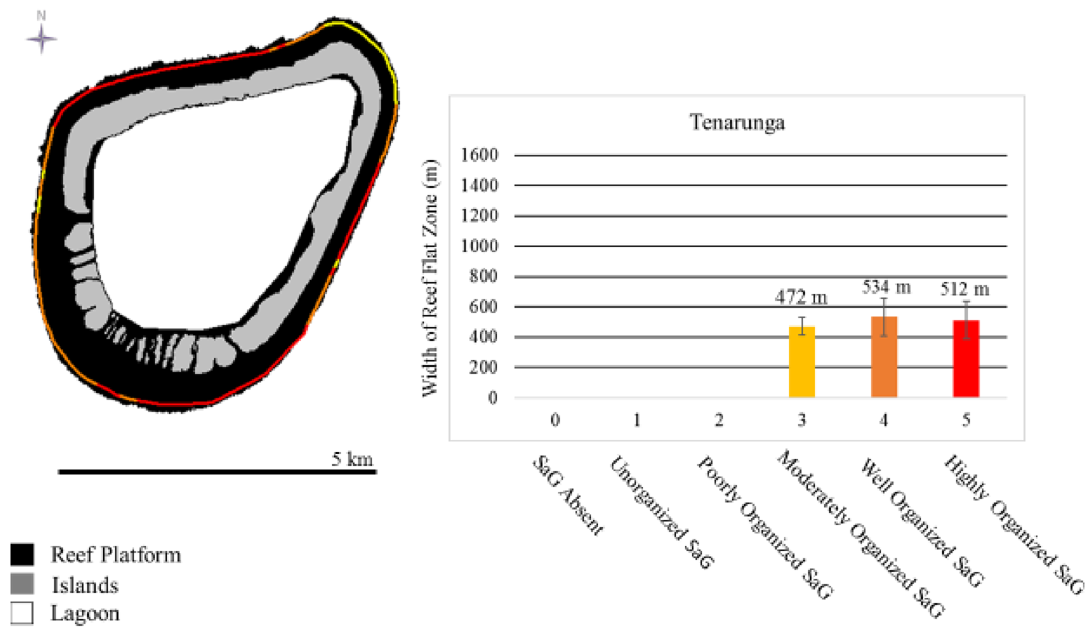


Figure 19. Graph showing relationship between RFZ width and Sag Ranking for Tenarunga

### 3.1.9 Bajo Nuevo

Bajo Nuevo did not show a consistent trend in the relationship between average RFZ width and the degree of the SaG development (Figure 20). SaG on Bajo Nuevo that was ranked with a 1 (n=22) corresponded to an average RFZ width of 417 meters. The RFZ average width for areas with SaG ranked 2 (n=17) went against the expected trend of increasing and instead decreased to 361 meters. However, the trend shifted once again as SaG ranked 3 (n=31) was associated with an average RFZ width of 450 meters. Continuing with that trend, SaG earning a ranking of 4 (n=47) also saw an increase in the adjacent average RFZ width with it being 1001 meters. However, that trend ended as SaG ranked 5 (n=205) was associated with an average RFZ width of only 762 meters.

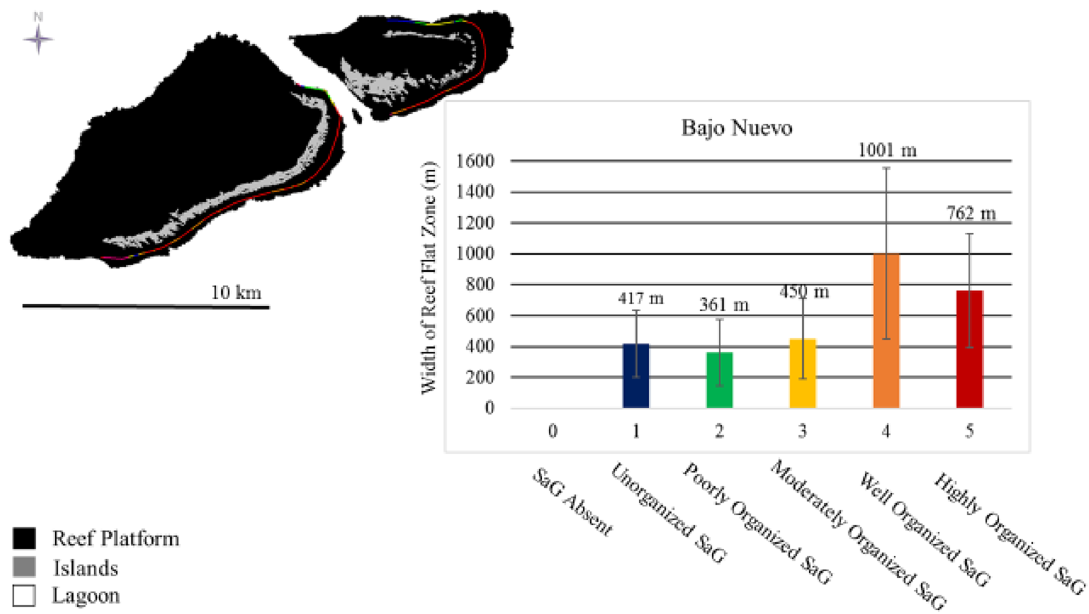


Figure 20. Graph showing relationship between RFZ width and SaG ranking for Bajo Nuevo.

## 3.1.10 Diego Garcia

As Figure 21 shows, Diego Garcia expressed an overall positive trend of average RFZ width in relation to the increase in SaG development, with only the exception of SaG ranked 3 (n=20) bucking from that trend. For the RFZ areas that lacked any SaG (n=43), the average width was recorded to be 634 meters. The average width of the RFZ increased to 674 meters when audited from areas adjacent to SaG which received a rank of 1 (n=50). The average RFZ width again increased, this time to 1018 meters, when associated with SaG that had a ranking of 2 (n=20). Oddly, the average RFZ width decreased to 804 meters for areas adjacent to SaG that was ranked 3 (n=70). However, this decrease in the average RFZ width did not begin a negative trend and where SaG received a ranking of 4 (n=105), RFZ increased back up to 1065 meters. Lastly, the widest average RFZ width, 1157 meters, was recorded from areas associated with SaG that was ranked 5 (n=361).

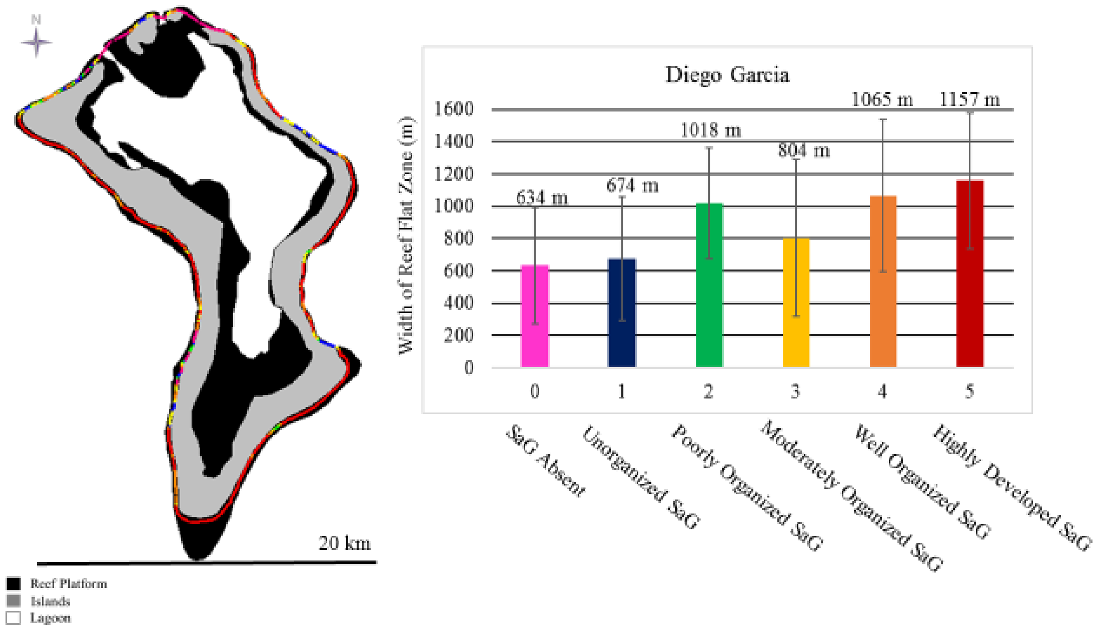


Figure 21. Graph showing relationship between RFZ width and SaG ranking for Diego Garcia.

## 3.2 Analysis of Well- to Highly-Developed SaG on Opposing Precincts and Their Statistical Significance

It is well known that the high energy on the exposed, windward margin of a carbonate platform creates the optimal area for well-developed SaG to exist (Blanchon and Jones, 1995; Gischler, 1995; Gischler and Lamano, 2000; Woodroffe et al., 2004; Kan et al., 1997). The results of the precinct analysis show that a majority of the sites fell in line with the current understanding of where on the platform SaG morphology expresses itself in regards to the windward, leeward, swellward, and swell-sheltered margins. As Table 3 shows, six out of the nine sites showed the expected result for the windward and leeward straight margins, eight out of nine sites showed the expected result for the swellward and swell-sheltered margins, and seven out of the nine sites showed the expected result for the windward and leeward promontories. The three smallest sites, Tenarunga, Motu One, and Mauhippa, did not act as expected in regards to the windward and leeward straight margins. These three sites were also the most circular when compared to the other six platform shapes. Palmerston, Diego Garcia, Bajo Nuevo, and Cook Reef were unique in that they were the only four sites that met the expectations of where well developed SaG should express themselves for all three precinct regions investigated (windward/leeward straight, swellward/swell-sheltered, and windward/leeward promontory). The two major metrics that these three sites all shared were their medium-large to large area and their angular shape.

Table 3. Table listing the margin which contained the greater percentage of Well- to Highly-Organized SaG. An asterisk (*) denotes that the margin listed is not statistically significant from its opposing margin. (WW: windward; LW: leeward; SW: Swellward; SS: swell-sheltered)

| | | | Margin Containing the Greater Percentage of Well- to Highly-Organized SaG | | |
|---|---|---|---|---|---|
| **Site Name** | **Platform Size (km$^2$)** | **Platform Shape** | **WW Straight vs. LW Straight** | **SW vs. SS** | **WW Promontory vs. LW Promontory** |
| Tenarunga | 13 | Teardrop | LW Straight | SW | LW Promontory |
| Motu One | 16 | Circular | LW Straight | SW* | WW Promontory* |
| Mauhippa | 60 | Smoothed Diamond | LW Straight | SW | WW Promontory |
| Palmerston | 64 | Diamond | WW Straight | SW | WW Promontory |
| Foa and Lafuka | 72 | Vertical Elongate | WW Straight | SW | LW Promontory* |
| Aitutaki | 103 | Trinangular | WW Straight | SS* | WW Promontory* |
| Diego Garcia | 190 | Double Tiered Diamond | WW Straight | SW | WW Promontory |
| Bajo Nuevo | 205 | Horizontal Elongate | WW Straight | SW | WW Promontory |
| Cook Reef | 380 | Vertical Elongate | WW Straight | SW | WW Promontory |

### 3.2.1. Cook Reef

As Figure 22 shows, 74% of the straight windward margin precinct was well- to highly-developed SaG. The straight leeward margin precinct was only comprised of 16% well- to highly-developed SaG. Binomial testing showed these two precincts to be significantly different. The same precincts were also used to decipher the swellward and swell-sheltered precincts, respectively. Therefore, the percentage of well- to highly-developed SaG and its statistical significance is also identical to the straight windward and leeward margin precincts. The windward promontory precinct contained 65% of well- to highly-developed SaG while the leeward promontory only contained 14% of well- to highly-developed SaG. Binomial testing showed these precincts to be statistically significantly different.

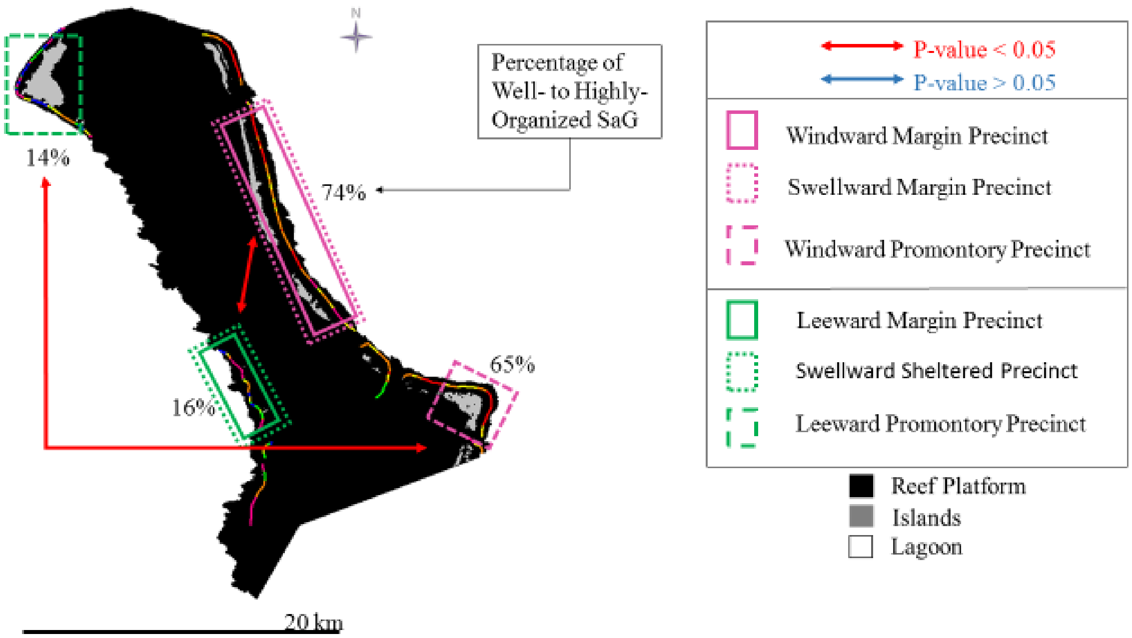


Figure 22. Precinct map for Cook Reef.

### 3.2.2 Foa and Lafuka

As Figure 23 shows, 74% of the SaG within the straight windward margin precinct was comprised of well- to highly-organized SaG. Comparatively, 50% of the straight leeward margin precinct contained well- to highly-organized SaG. Binomial testing showed these two precincts to be statistically significantly different. Due to similar wind and wave environments surrounding Foa and Lafuka, the windward precinct was also used as the swellward precinct while the leeward precinct was used as the swell-sheltered precinct. Therefore, the percentages of well- to highly-organized SaG and the significant difference remained the same. As for the windward promontory precinct, 68% of the SaG within that precinct was ranked well- to highly-organized. The leeward promontory was comprised of 69% well- to highly-organized SaG. Binomial testing showed that these two precincts were not significantly different.

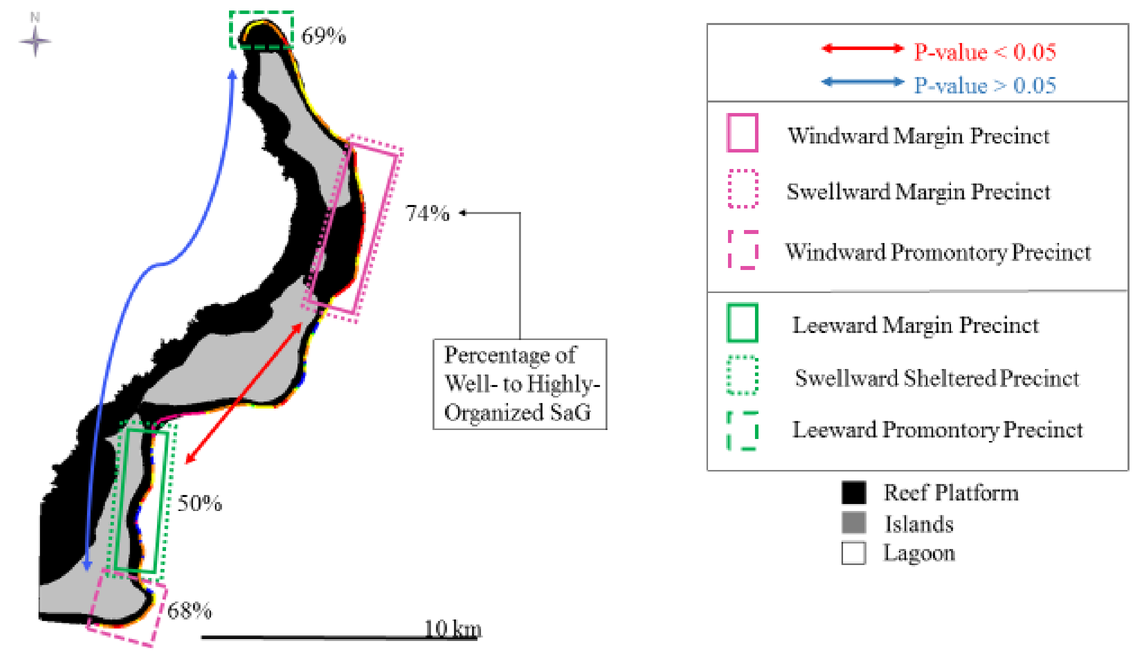


Figure 23. Precinct map for Foa and Lafuka Islands

### 3.2.3 Palmerston

As Figure 24 shows, the straight windward margin precinct of Palmerston contained 58% well- to highly-organized SaG. Comparatively, the leeward straight margin precinct contained no well- to highly-organized SaG. Binomial testing showed that these two precincts were statistically significantly different. The swellward precinct was comprised of 79% well- to highly-organized SaG. The swell-sheltered precinct, however, contained only 8% well- to highly-organized SaG. Again, binomial testing showed these two precincts to be statistically significantly different. Lastly, the windward promontory precinct contained 90% well- to highly-organized SaG whereas the leeward promontory was void of any well- to highly-organized SaG. These two precincts were also found to be significantly different.

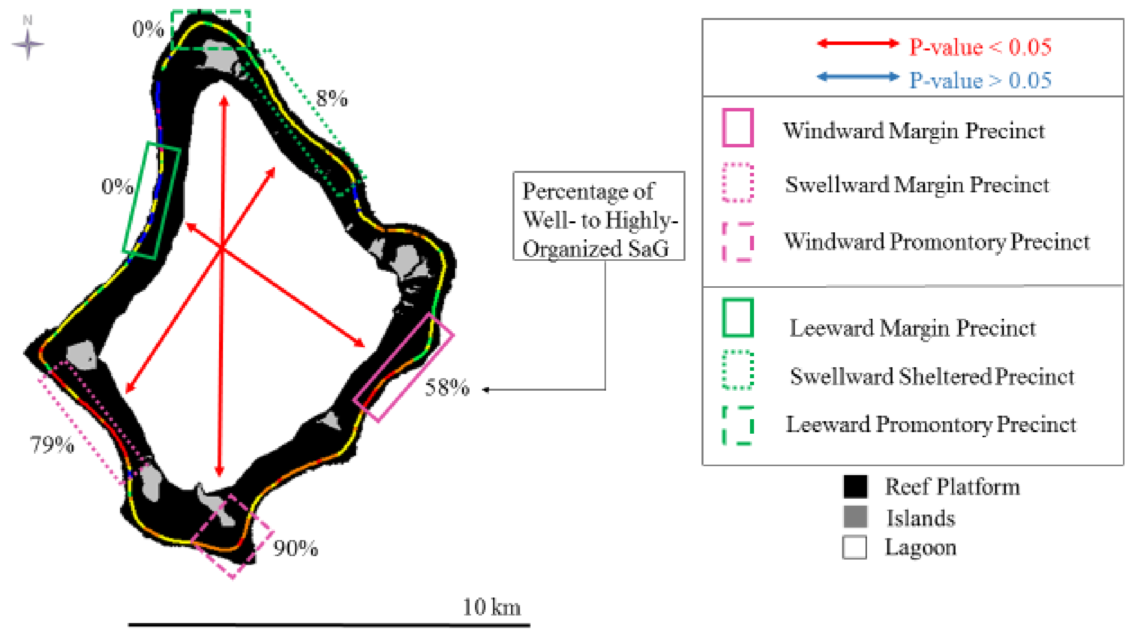


Figure 24. Precinct map for Palmerston.

### 3.2.4 Aitutaki

As Figure 25 shows, 67% of the SaG in the straight windward margin precinct of Aitutaki was well- to highly-organized. Comparatively, its opposing precinct only contained 15% SaG considered to be well- to highly-organized. The binomial testing done on these two precincts showed that there was a significant difference between the well- to highly-organized SaG. The swellward precinct contained 12% well- to highly-organized SaG, while the swell-sheltered precinct contained 24% well- to highly-organized SaG. Binomial testing showed that there was no significant difference between the two precincts. The windward promontory precinct of Aitutaki contained 32% well- to highly-organized SaG while the leeward promontory precinct contained only 18% well- to highly-organized SaG. Binomial testing showed that there was no significant difference between the percentages of well- to highly-organized SaG of these two precincts.

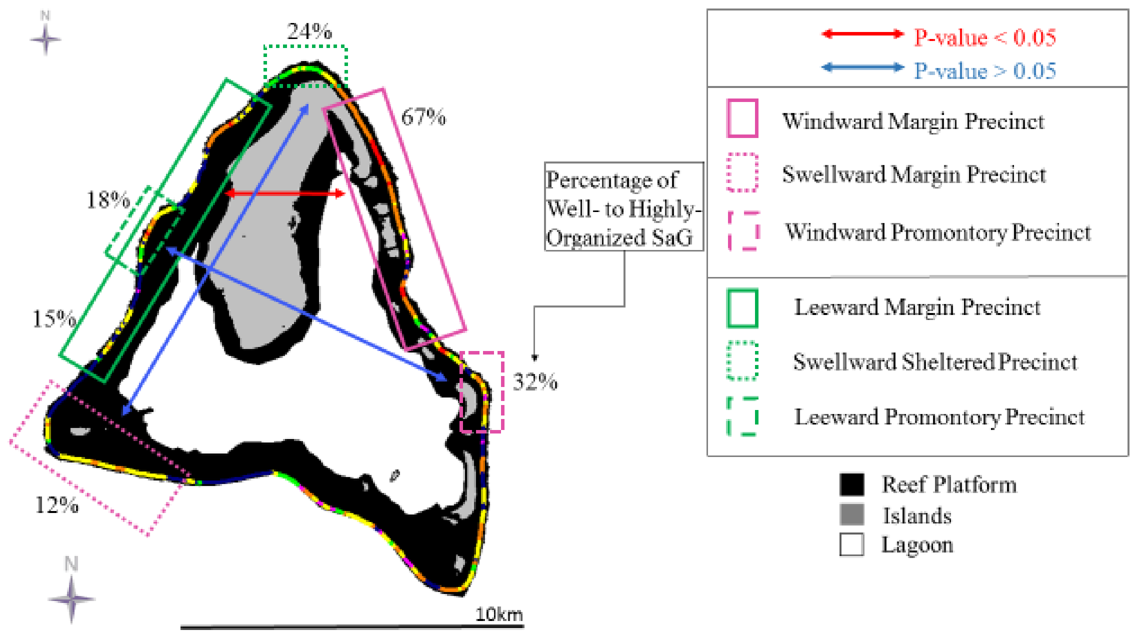


Figure 25. Precinct map for Aitutaki

### 3.2.5 Motu One

As Figure 26 shows, 76% of the SaG within the windward margin precinct of Motu One was that of well- to highly-organized. The leeward margin precinct, however, contained 93% well- to highly-organized SaG. Binomial testing showed that this difference, although not expected, was in fact statistically significantly different. The swellward precinct contained 90% well- to highly-organized SaG while the swell-protected precinct was comprised of 74% well- to highly-organized SaG. This was found to not be significantly different. The windward promontory margin contained 81% well- to highly-organized SaG while the leeward promontory only contained 65% well-to highly-organized SaG. Binomial testing found these two precincts to not be significantly different as well.

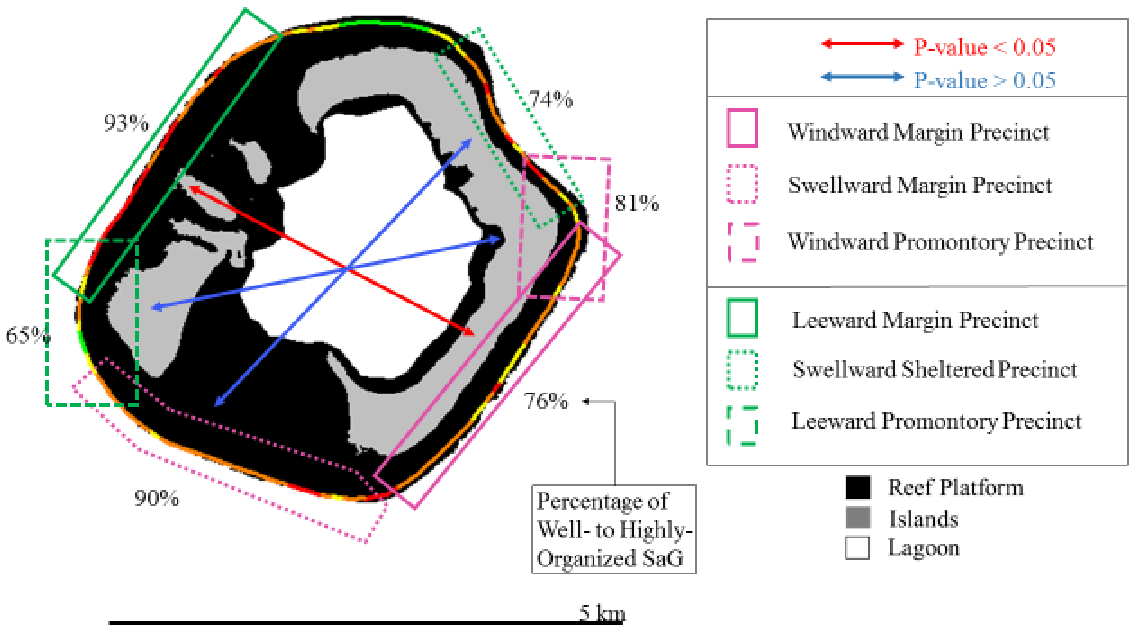


Figure 26. Precinct map for Motu One

### 3.2.6 Mauhippa

As Figure 27 shows, no well- to highly-developed SaG was found on the straight windward margin precinct and 33% of the straight leeward margin precinct was comprised of well- to highly-organized SaG. Through binomial testing these two precincts were shown to be significantly different. In the swellward precinct, 65% of the SaG there was ranked well- to highly-organized while the swell-sheltered precinct was void of any well- to highly-organized SaG. Binomial testing again showed that these two precincts were significantly different. The windward promontory precinct contained 54% well- to highly-developed SaG while the leeward promontory precinct contained 40% well- to highly-developed SaG. These two precincts were found to also be statistically significantly different.

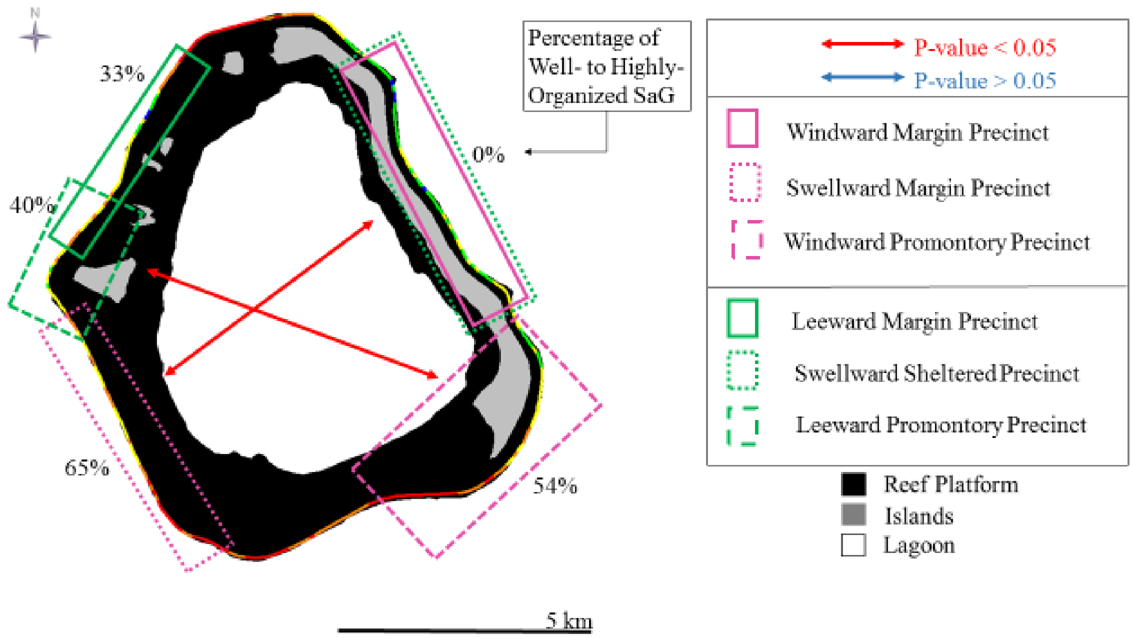


Figure 27. Precinct map for Mauhippa

### 3.2.7 Tenarunga

As Figure 28 shows, the straight windward precinct of Tenarunga contained 94% well- to highly-organized SaG while the straight leeward precinct was entirely comprised of well- to highly-organized SaG. Binomial testing showed that these two precincts were statistically significantly different. The swellward precinct contained 100% well- to highly-organized SaG while the swell-sheltered precinct only contained 12% well- to highly-organized SaG. Binomial testing found these two precincts to be significantly different as well. The way the wind and swell environment set up resulted in the swell-sheltered precinct of Tenarunga to also be the windward promontory precinct. Therefore, the windward promontory precinct also was recorded as containing 12% well- to highly-organized SaG while the leeward promontory precinct was entirely comprised of well- to highly-organized SaG. As previously stated, this was a statistically significant difference.

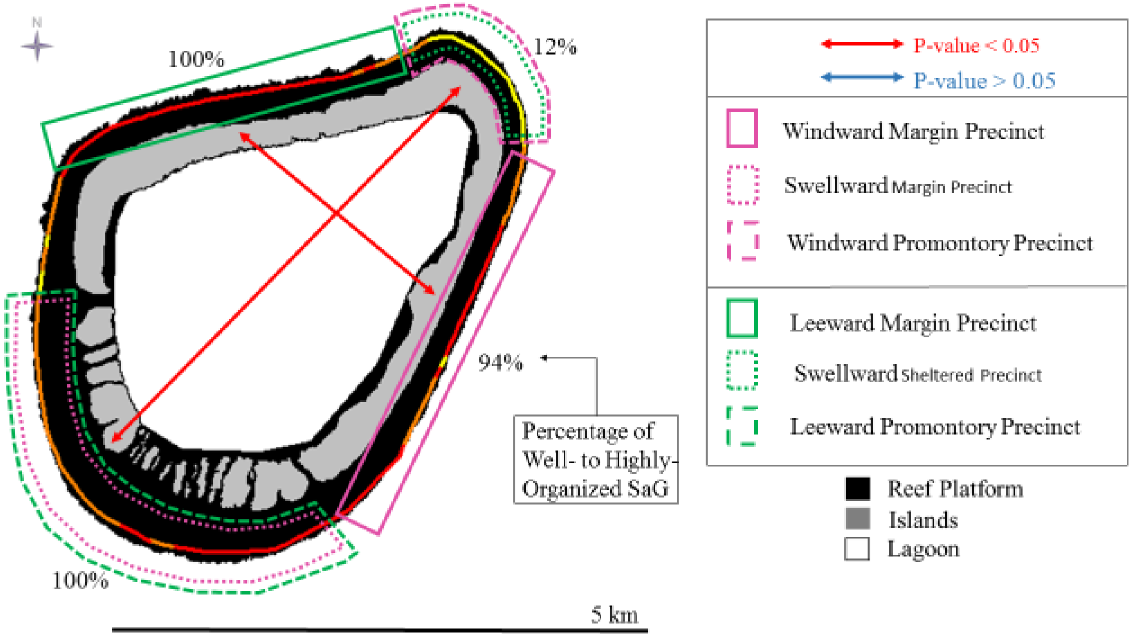


Figure 28. Precinct map for Tenarunga

### 3.2.8 Bajo Nuevo

As Figure 29 shows, 100% of the SaG found in the straight windward margin precinct of Bajo Nuevo was well- to highly-organized. Compared to its opposing leeward precinct, which contained no well- to highly-developed SaG, there was found to be a statistically significant difference between the two precincts. These precincts also served as being the swellward and swell-sheltered precincts, respectively. As with the windward and leeward precincts mentioned beforehand, the swellward precinct contained 100% well- to highly-organized SaG, while the swell-sheltered precinct contained no well- to highly-organized SaG. Binomial testing showed that there was a significant difference between the two precincts. Similarly, the windward promontory precinct was comprised 100% of well- to highly-organized SaG, while the leeward promontory did not contain any well- to highly-organized SaG. Binomial testing again showed that the differences between these precincts located on the windward and leeward promontories were significantly different.

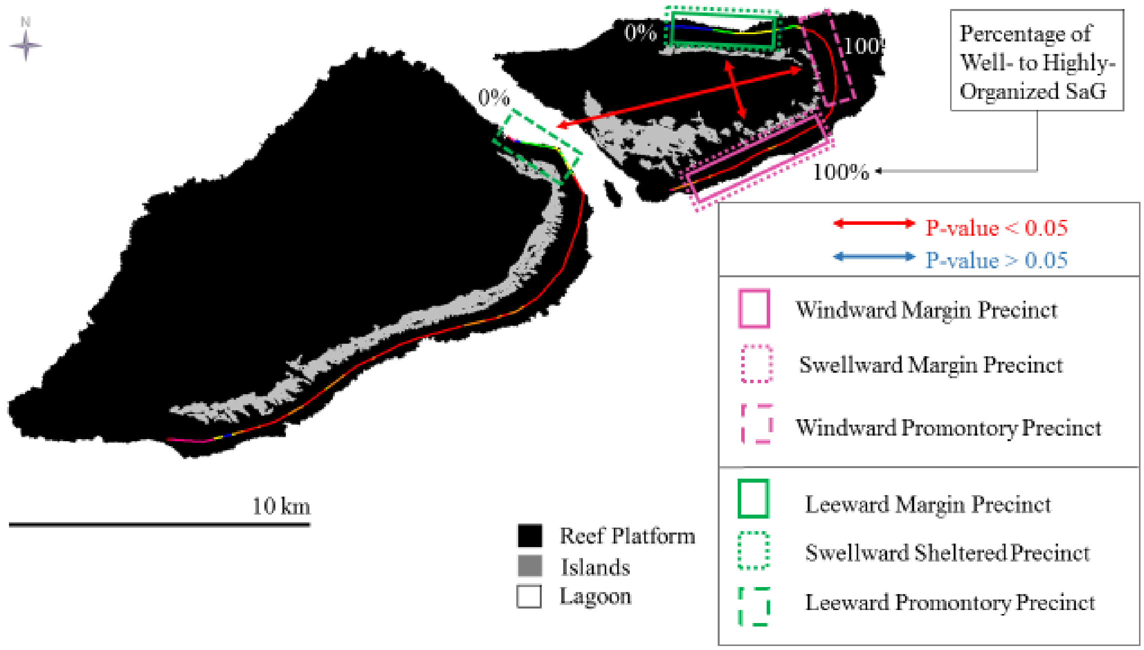


Figure 29. Precinct map for Bajo Nuevo

### 3.2.9 Diego Garcia

As Figure 30 shows, 97% of the SaG found in the straight windward margin precinct of Diego Garcia was well- to highly-organized. The straight leeward margin precinct, however, only contained 13% well- to highly-organized SaG. Binomial testing showed that this difference was a statistically significant difference. The swellward precinct of Deigo Garcia was comprised of 93% well- to highly-organized SaG while the swell-sheltered precinct only contained 28% well- to highly-organized SaG. These precincts were also found to be significantly different. Lastly, the windward promontory precinct contained 96% well- to highly-organized SaG, while the leeward promontory precinct only had 60% well- to highly-organized SaG. Binomial testing showed that the percentages of well- to highly-organized SaG was statistically significantly different.

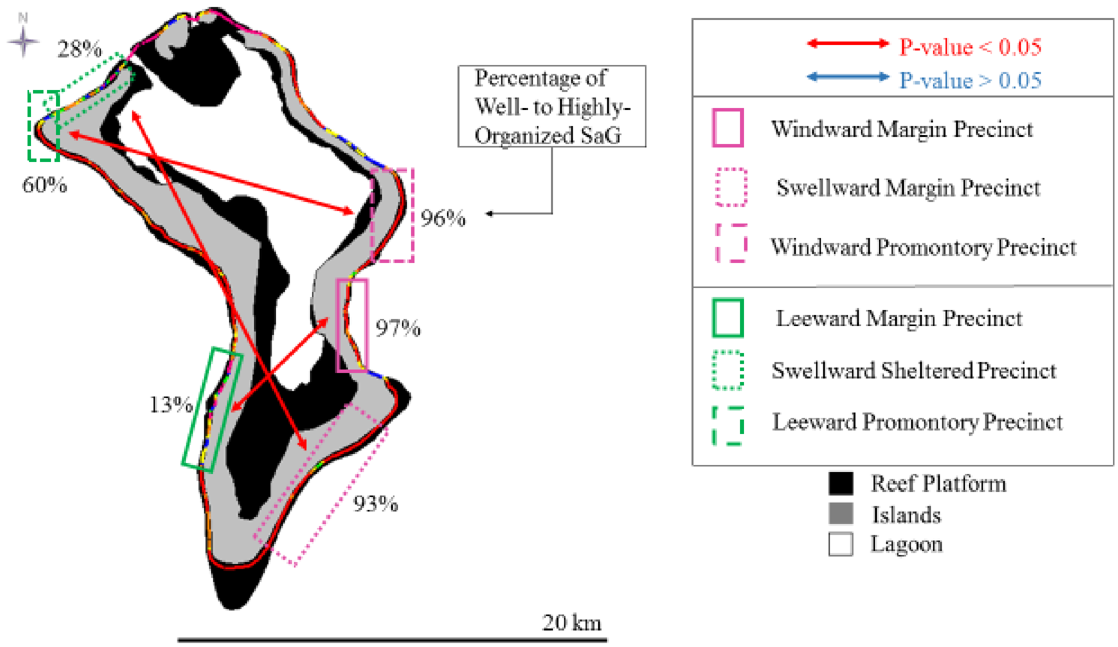


Figure 30. Precinct map for Diego Garcia

## 3.3 Interpretation of the Fast Fourier Transform's Primary Peak

The FFT primary peak showed the most frequently occurring spur width, in meters, found within the transect run through the FFT analysis. Using the results of the analysis and comparing the primary peak to the SaG from which the transect was taken, it was apparent that the width highlighted on the graph corresponded to the most common reoccurring spur width. Table 4 shows the primary peak values for SaG earning a 3, 4, and 5 ranking for each site. Results from the FFT showed that across all sites, the primary peaks for the transects run over SaG with a Ranking of 4, were most uniform with primary peaks only ranging between 4.4 and 9.2 meters**.** Five of these nine sites had primary peaks between 5.7 and 7.1 meters. Primary peaks from the transects run across SaG with a ranking of 5 were the next in the order of uniformity. Foa and Lafuka Islands was the only site that did not have a SaG Ranking of 5 and not included in this assessment. However, for the remaining eight sites that did have SaG ranked 5, the primary peaks ranged from 6 meters to 16 meters with six sites having a primary peak between 6.0 and 9.5 meters. The most unorganized spattering of primary peaks came from the FFT ran over SaG with a ranking of 3. The range of these peaks spanned from 2 meters to 19 meters. Three sites had primary peaks of less than 5 meters, two sites had primary peaks that fell in between the 5 to 10 meter range, and four sites had primary peaks that were between 14 and 19 meters.

Table 4. Table Highlighting the Fast Fourier Transform's Primary Peak, in meters, for SaG Ranked 3, 4, and 5 at each site.

| Site Name | Platform Size ($km^2$) | Platform Shape | FFT PP (m) for SaG Ranked 3 | FFT PP (m) for SaG Ranked 4 | FFT PP (m) for SaG Ranked 5 |
|---|---|---|---|---|---|
| Tenarunga | 13 | Teardrop | 9.7 | 9.2 | 7.8 |
| Motu One | 16 | Circular | 6.4 | 8.2 | 6 |
| Mauhippa | 60 | Smoothed Diamond | 2.2 | 4.4 | 9.5 |
| Palmerston | 64 | Diamond | 19 | 6.7 | 7.7 |
| Foa and Lafuka | 72 | Vertical Elongate | 3.2 | 5.7 | N/A |
| Aitutaki | 103 | Triangular | 16.4 | 6.5 | 6.9 |
| Diego Garcia | 190 | Double Tiered Diamond | 5 | 7.1 | 12.7 |
| Bajo Nuevo | 205 | Horizontal Elongate | 15.5 | 6.7 | 8.5 |
| Cook Reef | 380 | Vertical Elongate | 14.6 | 8.6 | 16.5 |

## 3.4 Results of Current Analysis

Plotting the date and the corresponding average direction of the currents offered an easy way to visually investigate any seasonal current trends (see Appendix A). This method also allowed for individual analysis on a site by site basis.

### 3.4.1 Cook Reef

Cook Reef only showed to have similar current directionality for the months of October and December for 2006 and 2008. The other months from the two years did not line up with the each other in such a way to be labeled as sharing the same directionality.

### 3.4.2 Foa and Lafuka Islands

Foa and Lafuka Islands showed similar current directionality for January, March, and June of 2006 and 2008. August, October, and December did not share in this consistency between the two years audited.

### 3.4.3 Palmerston

Palmerston only showed similar current directionality for one month, August, between the two years audited. The other months differed too much in direction between the two years to attribute any consistent current directionality.

### 3.4.4 Aitutaki

Aitutaki showed little consistency with current directionality between 2006 and 2008. Out of the six months of the year selected, only June, August, and October shared the same current direction. The other months, January, March, and December varied too much with their directions to show a strong seasonal trend.

### 3.4.5 Motu One

Motu One showed similar current directionality for the months of June, August, and October. However, the other three months that were included in this two-year comparison, January, March, and December, did not maintain their directionality from 2006 to 2008.

### 3.4.6 Mauhippa

Mauhippa showed no consistency between 2006 and 2008 for any of the months audited. A seasonal trend in current directionality could not be determined for the available data.

### 3.4.7 Tenarunga

Tenarunga showed no current direction consistency for any month for the two years audited. Each month in 2008 differed from its 2006 counterpart by at least 100 degrees with December showing a difference of 245 degrees. Therefore, no seasonal prevalence could be determined.

### 3.4.8 Bajo Nuevo

Bajo Nuevo showed similar current directionality for the months of January, June, August, and December for 2006 and 2008. March and October for those two years varied too greatly to say that currents consistently come from the same direction during those months.

### 3.4.9 Diego Garcia

Diego Garcia showed season trends in current direction by having similar directional readings for the years 2006 and 2008 for the months of January, August, October, and December.  The months of March and June differed too much in the two years audited to determine the prevalent direction of the currents during those months.

# 4 Discussion

Given the multifaceted nature of this study in how it looked at spur and groove organization and development, factors that contributed to that organization, and how the degree of organization influenced Reef Flat Zone size, it was no easy task to extricate the tangled relationships existing between all the variables.

## 4.1 The Relationship between SaG Rank and the Adjacent Reef Flat Zone

It was hypothesized in this study that well-organized SaG would be associated with the wider sections of Reef Flat Zone (RFZ) of an atoll or island. In an idealized scenario, as SaG development increases, more efficient sediment channels would arise which would supply the RFZ with the needed sediment to accrete at the shoreward end of the groove. Of the nine sites investigated for this study, Mauhippa had the strongest trend of SaG ranking increasing as RFZ width increased along with it (Table 2). Motu One, Palmerston, and Tenarunga also had similar, positive trends.  With Tenarunga being 13 sq. kilometers, Motu One being 16 sq. kilometers, Mauhippa being 60 sq. kilometers, and Palmerston being 64 sq. kilometers, these four sites fall in the small to medium size range relative to all sites surveyed.  Palmerston and Mauhippa both are categorized as having a shape similar to that of a diamond.  Motu One and Tenarunga on the other hand, are more circular in shape. Results suggest that these two shapes lend themselves to being the most advantageous for well-organized SaG to form and contribute to increasing the width of the RFZ.  Incoming hydrodynamic energy is a major driving force behind SaG development (Rogers, et al. 2013; Monk and Sargent, 1948, Shinn, 1963, and others). Having well organized SaG is crucial in supplying the RFZ with sediment needed for expansion (Goureau, 1959; Shannon et al., 2012; O’Leary and Perry 2012; Smithers and Hopley, 2006). The size and shape of the atoll also has an influence on the incoming energy being dispersed around the atoll and in turn, the development of SaG around an entire island is tied in part to the size and shape of the atoll (Mendelier and Kench, 2012; Robert 1974). Circular atolls appear to have an efficient response to dispersing this energy and therefore can have a better SaG organization spanning the entire perimeter of the island (Reese et al., 2006; Kan et al. 1997). Larger sites may be completely devoid of any SaG or any well-developed SaG on leeward or sheltered areas and therefore will not benefit from the sediment channeling abilities of the SaG (Kan et al. 1991; 1997; Woodroffe et al., 2004). Of the sites investigated in this study, the size and shape that may be most conducive to advanced SaG development and organization and therefore proper channels for sediment movement is an atoll between 10 and 65 sq. kilometers and taking a curved, circular form or a diamond form with softened corners. This finding implies that the long shores of the larger sites that sit perpendicular to the incoming wave energy block rather than disperse and refract incoming energy. This prevents the positive feedback mechanisms needed to establish a strong SaG network and therefore results in a spattering of SaG development aligning with sections of the RFZ seemingly uninfluenced by the channeling properties of the SaG.

Another aspect of RFZ width to take into account is how the atoll was initialized. Of course, not all of the sites started off with an initial reef crest of the same width. Some islands in these regions may have started off with wider RFZ's than others and some may have had a temporal head start in development. Another point to consider is that different sites may have inherited different degrees of antecedent topography from previous sea level highstands and therefore the RFZ width observed on the satellite imagery is not genuinely reflective of modern observable conditions. Sites meeting that criteria are referred to as pinned atolls (Shinn et al., 1981; Rankey et al., 2009). Sediment cores and dating would be needed in order to recreate the history of each site and come to a common starting point from which all sites could be equally judged. Therefore, given the sheer scope of this study, I could not take into consideration all the different nuances that could have played a role in making a baseline estimate of initial RFZ width. My study could only infer, based of the uncovered relationship between the SaG rankings and RFZ width, that well-organized SaG appears to be a conduit for sediment to be transported onto the RFZ, enabling the possibility to enhance the RFZ width over time.

## 4.2 Analysis of the Statistical Significance of Well Organized SaG on Opposing Platform Margins

The degree to which SaG is expressed on windward versus leeward and swellward versus swell-sheltered margins was another major aspect of this study. It is well known that SaG formation can be molded by hydrodynamics on the reef flat margins and that the margins exposed to the incoming energy over an environment more conducive for SaG development (Yamano et al., 2003; Mendelier and Kench, 2012; Roberts, 1974; Hongo and Kayanne, 2008). However, there was a need to further investigate how reef platform shape influenced SaG exposure to these hydrodynamic forces and in turn how that may determine where well-organized SaG express itself on the platform. Due to highly-developed SaG (Ranking of 4 and 5) being the SaG most vital for sediment nourishment onto and off of the RFZ due to the well carved grooves, these SaG were chosen to be analyzed.

### 4.2.1 The Exception of Tenarunga and Motu One

SaG forms under the guidance of hydrodynamics set up by prevailing winds (Shaked et al., 2003; Grigg, 1998; Blanchon and Jones, 1995; Gischler, 1995; Gischler and Lamano, 2000). Therefore, one would expect to see the more organized SaG dominate the windward margin of a site while the leeward side would not express SaG to the same degree. However, Tenarunga and Motu One do not showcase this expected outcome. In Tenarunga's case, not only does the straight leeward margin contain better developed SaG than the windward margin, rather it is 100% comprised of highly developed SaG. Also, the windward promontory contains only 12% well developed SaG while the leeward promontory side contains 100% well organized SaG (Figure 28). It is important to note that because of the circular, teardrop shape of Tenarunga and the surrounding wind and wave environments, the windward promontory precinct also doubles as the swellward precinct while the leeward promontory precinct doubles as the swell sheltered precinct. Tenarunga's size and shape are two factors that might play into this unique expression of SaG around the atoll. Smaller, circular sites allow for energy refraction around the entire site therefore diminishing any assumed discrepancies between the windward and leeward margins (Reese et al. 2006; Kan et al. 1997). This led to Tenarunga being only comprised of SaG which ranked at 3, 4, and 5. Tenarunga was the only site where the lowest ranking was a three, a moderately organized and developed expanse of SaG, and it should be noted that there were no recorded gaps in SaG continuity around the island.

Motu One was similar to Tenarunga in that the expected preference for SaG to be better developed on windward and swellward margins as opposed to their leeward and swell-sheltered counterparts was not the case. Not only did opposing margins share similar percentages of well- to highly-developed SaG, but the binomial testing of the results that did follow the expected trend proved to not be statistically significant. Like Tenarunga, Motu One is a small (13 sq. km) atoll but is nearly perfectly circular (Figure 3). The circular shape facilitates the refraction wave energy (Adams and Haslerr, 2010; Mendelier and Kench, 2012). In doing so, the role that margins play in establishing a predominant windward and leeward sides to the atoll are diminished as all sides receive SaG shaping energy. This results in well- to highly-organized SAG being expressed on all sides of the atoll.

### 4.2.2 Why Aitutaki Did Not Align with Expectations

Aitutaki's triangular shape and relativity large (103 sq. km) area partially explains why its swellward and windward promontory precincts do not align with expected results of a margin exposed to the incoming energy. Because the swell is coming in from the south southwest (Figure 3), its energy is concentrated at that convex section on its southern margin and that may create a situation where refracted waves are canceling each other out and do not have an opportunity to focus potential energy in a consistent enough manner to play a large role in the creation and maintenance of SaG. This results in only 12% of the SaG in that southwest region of the Aitutaki being well- to highly-developed (Figure 25). This region's opposing precinct, located at the northern tip of the triangularly shape atoll and more exposed to the year-round wind, may be subjected to the wind waves generated by incoming energy traveling alongshore. The windward margin is 16 km in length, creating a relatively long obstruction perpendicular to the prevailing winds of the region. While this certainly would provide the statistically significant difference in the amount of well- to highly-developed SaG from windward to leeward margin, I propose it may also have to do with influencing the percentage of SaG located within the swell sheltered precinct. Aitutaki's triangular shape may come into play again when looking at the amount of well- to highly-developed SaG that occupy the windward promontory precinct as well. This southeastern promontory did provide an area that jutted out into the oncoming wind and wave energy. However, perhaps in a similar fashion to the southwestern swellward promontory mentioned earlier, the relatively sharp angle of this promontory could be what kept the amount of well- to highly- organized SaG to only make up less than one third of windward promontory precinct. Also, the fact that there was no statistical significance between the windward promontory and the leeward promontory may point to the unique triangular shape having an unpredictable influence on the refraction of wind waves.

### 4.2.3 Ideal Platform Shapes and Sizes That Display Margin Specific SaG Development

There were four sites (Palmerston, Diego Garcia, Bajo Nuevo, and Cook Reef) that offered the ideal results in terms of how the expected prevalence of SaG development would differ along the various energy influenced margins of the atoll. All four sites were shown to have the windward and swellward precincts contain significantly more well- to highly-organized SaG and through binomial testing it was shown that these were statistically significant results (Table 3). Common aspects these four sites shared were that they were all very angular, had long stretches of a "straightaway" margin, and with the exception of Palmerston, were all greater than 190 sq. km. Palmerston was of the medium sized sites (64 sq. km) but it was the most angular of them all (Figure 3). The angularity of Palmerston may have made up for its lack of relative size in terms of explaining how it maintained a sharp distinction between the amount of well- to highly-organized SaG on windward and leeward margins. It would not be hard to imagine that an atoll containing distinct margins parallel and perpendicular to the incoming wave and swell energy could serve the same purpose as having just one very long margin blocking incoming wave energy from refracting to the other side or having a very large, curving promontory collecting the incoming energy and not allowing it to continue on around to the leeward and sheltered side as appears to be the case at Cook Reef.

### 4.2.4 The Unique Case of Foa and Lafuka Islands

Foa and Lafuka Islands were unique in this study due to their geology and development as seen from satellite imagery. There were no SaG present on the literal leeward margin of the islands. Therefore, in this case, the “leeward” margins were attributed the more sheltered areas of the windward and swellward side of Foa and Lafuka Islands (Figure 23). The dominant windward precinct did have a significantly higher amount of well-to highly-organized SaG present compared to its more sheltered windward counterpart which took the name of “leeward” for this particular investigation. Foa and Lafuka offer a good look into the effects a protruding promontory has on reaping the hydrodynamic benefits of incoming oceanic energy for SaG development compared to other surrounding areas of the island that only receive more refracted and reflected wave energy.

### 4.2.5 Why Mauhippa Acts as an Outlier

Mauhippa had no well- to highly-organized SaG on its windward straightaway margin, while one third of the leeward margin counterpart was comprised of well-to highly-organized SaG (Figure 27). As it has been stated that SaG development and organization is a product of both wind and swell energy (Grigg 1998; Blanchon and Jones, 1995; Kan et al., 1991; 1997), it is surprising that a windward margin be void of any well-organized SaG from a satellite audit. A limiting factor in this study was the quality of the imagery used to conduct the visual investigation into the spatial parameters of the SaG. For this particular site, there was no amount of band stretching or image manipulation, or image enhancement that could take away the obstruction caused by the crashing waves in the high energy area of the atoll where SaG can be found (Figure 31). No other imagery was available that offered the resolution needed to keep SaG measurement consistent with other sites of this study. On the windward promontory, the significant difference in more well-to highly-developed SaG is consistent with expectations of windward margins resulting in better developed and organized SaG. That finding lends itself to the notion that the hydrodynamics and SaG development were operating in an expected manner on Mauhippa and there may have been well-to highly-organized SaG hidden beneath the obstruction of the waves on the windward straightaway margin that were unable to be accounted for.

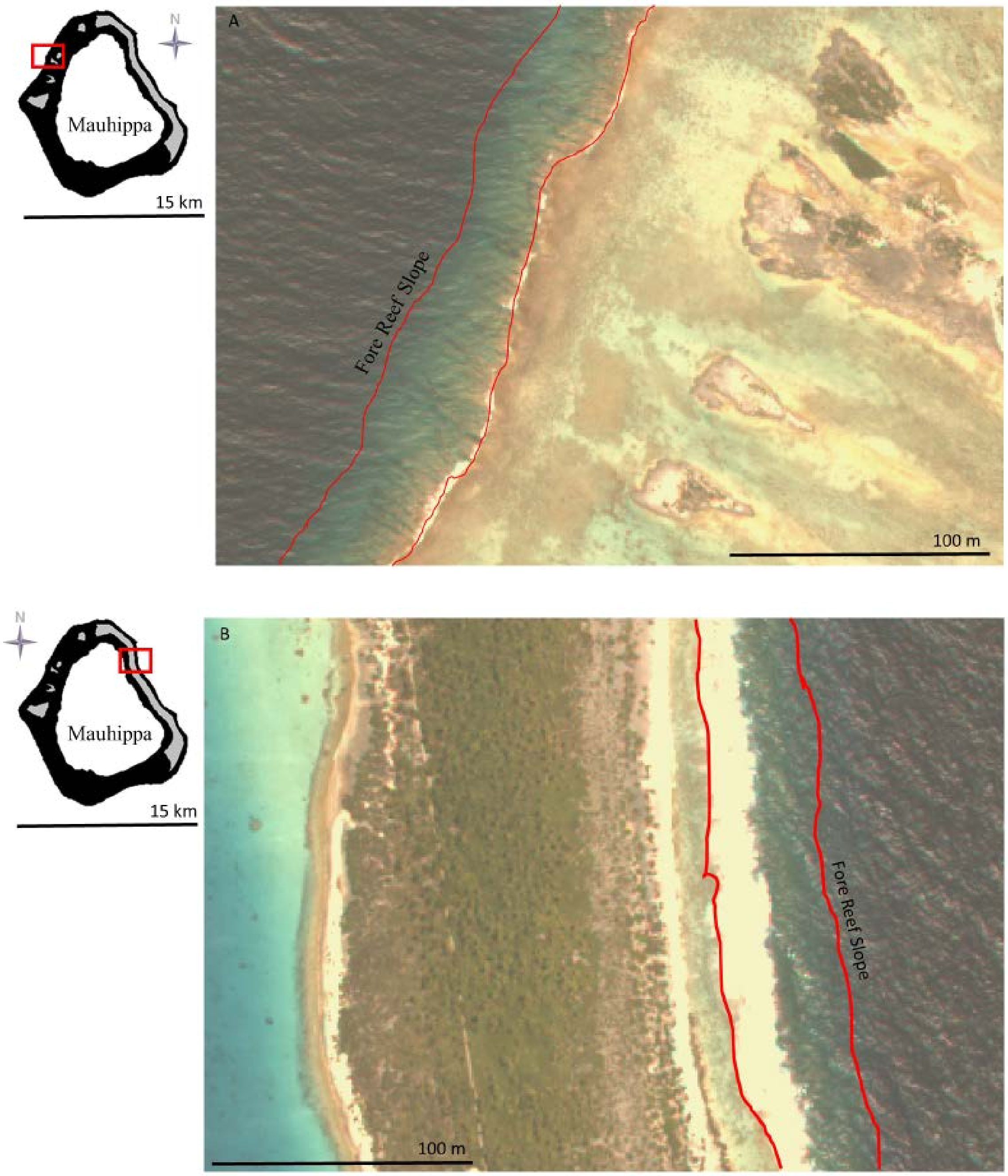


Figure 31. A) World View 2 satellite imagery showing an area of unobstructed Fore Reef Slope used to audit SaG. B) On the other side of the lagoon, crashing waves obstruct the Fore Reef Slope making SaG investigation impossible.

## 4.3 The Effects of Currents on SaG Organization and Development

The limited amount of data for the directionality of the currents and their rate of speed surrounding each study area were not enough to strongly suggest that the currents were persistent enough to have an impact on formation or maintenance of spur and groove morphology. Also, it is difficult parse the specific role currents play in an area of the platform margin where high energy waves dominate (personal communication, Purkis 2017). Access to additional current data that give insight into the hydrodynamics in the SaG zone may have been able show a seasonal trend in these areas. Persistent currents could, in theory, help set up the necessary hydrodynamics needed to keep grooves clear and supply the spurs with nutrient rich water to support coral growth.

## 4.4 Platform Size and Shape and Its Connection to the SaG Rank – FFT Primary Peak Relationship

The average FFT primary peak value (the most common reoccurring spur width) across all sites for SaG ranked 4 and 5, was 8.67 meters. I hypothesize that there are two trends to look for when investigating the relationship between the SaG Rank and the FFT Primary Peak (FFT PP). First, the trend of the FFT PP as SaG ranking increases should either progress or regress, towards the aforementioned FFT PP of well-developed SaG (8.67 meters). For example, take a SaG Ranked 3 with a hypothetical FFT PP of 13 meters. The expected trend in this scenario would be that the SaG ranked 4 have an FFT PP lower than 13, and the SaG ranked 5 should have an even lower FFT PP closer to that of 8.67 meters. SaG showing an increase in FFT PP from SaG ranked 3 to 5 is the complementary version of this trend and could also be expected depending on where the moderately organized SaG begins with its FFT PP. The main takeaway here is that as SaG becomes more developed and organized, the FFT PP closes in on the average width of well- to highly-developed spurs. To further investigate the role that the size and shape of a platform plays in determining SaG development and organization around an atoll, it was of interest to see how my aforementioned hypothesis on FFT PP was impacted given the different combinations of both platform size and shape of these differing sites.

The two smallest and most circular sites in this study, Tenarunga and Motu One, were the only two sites that showed an FFT PP that actually held consistent at each ranking investigated: 3, 4, and 5 (Table 4). This absence of any real trend was not expected but it was of interest to note that the observed FFT PP was near the average FFT PP of well- to highly-developed SaG. As shown in Table 4 Tenarunga, had an FFT PP of 9.7 meters for SaG Ranked 3, 9.2 meters for SaG Ranked 4, and 7.8 meters for SaG Ranked 5. Motu One showed an FFT PP of 6.4 meters for SaG Ranked 3, 8.2 meters for SaG Ranked 4, and 6.0 meters for SaG Ranked 5. As this unique relationship across the three rankings was only present in these two sites, it may point to small, circular platforms allowing for an underlying degree of developmental uniformity within the SaG that is missed by the more visually apparent variations in the different degrees of SaG organization.

Mauhippa, which is a medium sized (60 sq. kilometers) smoothed diamond shaped platform, displayed an ideal trend of increasing FFT PP as SaG rank increased (Table 4). SaG ranked 3 had an FFT PP of 2.2 meters and it gradually increased to 4.4 meters for SaG ranked 4, and lastly to 9.5 meters for SaG ranked 5. The only other site that displayed this trend was Diego Garcia (Table 4). Although they differ vastly in size, they do share a similar generalized geometry (Figure 3). Diego Garcia somewhat looks like a combination of two Mauhippa atolls, stacked atop one another. Because the trend exists in both sites while their size greatly differs, I argue that the shape of the platform may be the more important of the two variables in determining how SaG expresses itself around the platform.

The next observable trend was that shared between Palmerston and Aitutaki (Table 4). Palmerston is of the medium-large size at 64 sq. km while Aitutaki is of the large size at 103 sq. km. However, they both share the fact that they are very angular (Figure 3). Similar to how Diego Garcia was essentially two versions of Mauhippa stacked atop one another, Palmerston is similar to combining two Aitutakis. Aitutaki most closely represents a triangle in shape whereas Palmerston is that of a diamond. The trend that these two shared, as seen in Table 4, was that their SaG ranked as a 3 had a high FFT PP which then drastically dropped for SaG ranked 4. From there, the FFT PP then rose closer to the average FFT PP for well- to highly-developed SaG. Again, not unlike Mauhippa and Diego Garcia, a vast difference in area of the platform seems to be erased by the similarity in shape.

The two elongate sites, Foa and Lafuka Islands and Cook Reef, did not share any trend (Table 4). Cook Reef is nearly five times the size of the Foa and Lafuka Islands in terms of area, which may be too large of a difference in area for similarities in the geometric shape of the platform to be of any significance. While Foa and Lafuka Islands are missing SaG ranked 5, it should be noted that they were showing in increasing trend in FFT PP with increasing SaG Rank whereas Cook Reef started off with a very high FFT PP at 14. 6 meters for SaG Ranked 3, which then dropped down to 8.6 meters, and then nearly doubled to an FFT PP of 16.6 meters SaG ranked 5.

Lastly, Bajo Nuevo was the only site investigated in this study with its unique platform shape. It shared a similar trend as expressed on Aitutaki and Palmerston. That shared trend is a variation of the decreasing FFT PP from a high FFT PP for SaG ranked 3, down to the average spur width of well- to highly developed SaG. (Table 4). With no other horizontally elongate sites situated the way Bajo Nuevo is in regard to the surrounding oceanographic conditions, it is difficult to determine what role, if any, the size or more importantly the shape, has in establishing the aforementioned hypothesized ideal relationship between SaG Rank and FFT PP.

## 5. Conclusion

Understanding the physical parameters which control SaG development and organization adds to the current understanding of overall SaG morphology and how it interacts with its surrounding wind wave and swell environment. Yamano et al. (2003) called for a study that investigated reef morphology on islands of varying size that developed independently of one another. Motivated by Yamano et al. (2013), it was important for my study to combine different platform sizes and shapes, situated in various ocean environments around the globe to create a wide range of combination of factors in order to identify the strongest trends that bridged these different variables.

This study revealed the platform size preferential to the creation and establishment of well-developed and well-organized SaG morphology that could play a fundamental role in supplying the RFZ with sediment. Small to medium sized platforms (13 to 60 sq. kilometers) were found to exhibit a strong relationship between an increase in average RFZ width as SaG rank increased. This is most likely due to the ability of swell and wind waves to easily encompass the platform and deliver hydrodynamic forces used to shape SaG morphology. This study also found the most efficient platform shape where average RFZ width is found to grow wider as adjacent SaG becomes more developed and organized. Circular and diamond shape are the two best platform shapes needed to create a well- to highly-organized sections of SaG that can act as conduits for sediment transport. Small and medium platforms that are of the circular and diamond shape, allow for a strong positive feedback loop to form. This positive feedback loop consists of SaG formations able to become well- to highly-organized around much of the platform and thus nourishing the RFZ. One shortcoming of this study was not having the data needed to properly reconstruct the origin of each site to better understand what the width of the RFZ may have been when it first became subaerially exposed. This study added more evidence to the argument put forth by Kan et al. (1997), Reese et al. (2006), Woodroffe et al. (2004), and others that windward and swellward margins will host SaG morphology spanning multiple degrees of organization at a higher occurrence more often than their leeward counterparts. It was also noted that the larger and more angular a platform is, the more pronounced the difference will be in regards to windward and leeward preference for SaG morphology to express itself on the platform margin. Also, it appears that the size of the platform be can supplemented by the platform’s angularity to still maintain the sharp contrast of a highly-organized SaG dominated windward margin versus a SaG lacking leeward margin. That is to say, I argue that an angular platform will have more defined windward and leeward SaG development versus a circular platform of the same size. Lastly, the FFT analysis showed that a circular platform could share spatial organization across well- to highly-organized ranked SaG while other platform shapes would have a high primary peak for well-organized SaG and lower primary peaks for highly-organized SaG.

Further research, as suggested by Duce et al. (2016), would be crucial in further understanding just how various physical processes help influence the organization and development of SaG morphology on platform margins of shapes and sizes not included in my study. Also, having a better understanding of the width of an atoll's RFZ when it was first subaerially exposed and susceptible to sediment nourishment via SaG morphology would give more weight to the findings within this study. Having a better way to assess the on and off platform transport of reefal sediment could potentially help reinforce my hypothesis on what ideal SaG development and organization looks like through a more quantitative lens. Duce et al. (2016) focused on reefs within the Great Barrier Reef and mentioned how a larger scale investigation into SaG geomorphology could be beneficial to understanding nuances in the geomorphic development of SaG. My investigation into the physical parameters and constraints of what shapes and influences SaG morphology across at a global scale helps fill in voids of previous SaG studies.

## References


Abbey, E., Webster, J., Beaman, R., (2011). Geomorphology of submerged reefs on the shelf edge of the Great Barrier Reef: The influence of oscillating Pleistocene sea-levels. *Marine Geology* 288, 61–78

Andréfouët, S., Cabioch, G., Flamand, B., (2009). A reappraisal of the diversity of geomorphological and genetic processes of New Caledonian coral reefs: a synthesis from optical remote sensing, coring and acoustic multibeam observations. *Coral Reefs* (2009) 28, 691-707

Blanchon, P., Jones, B., (1995) Marine-Planation Terraces on the Shelf Around Grand Cayman: A Result of Stepped Holocene Sea-Level Rise. *Coastal Research* 11, 1-33

Cabioch, G.,Camoin, F., Montaggioni, L. (1999). Postglacial growth history of a French Polynesian barrier reef tract, Tahiti, central Pacific. *Sedimentology* 46, 985-1000

Edmonds, D., Paola, C., Hoyal, D., Sheets, B., (2011). Quantitative metrics that describe river deltas and their channel networks. Geophysical Research 116, 1-16

Ford, M., Kench, P., (2004). Formation and adjustment of typhoon-impacted reef islands interpreted from remote imagery: Nadikdik Atoll, Marshall Islands, *Geomorphology* (2014)

Gourlay, M., (1988). Coral Cays: Products of Wave Action and Geological Processes in a Biogenic Environment. *Proceedings of 6$^{th}$ International Coral Reef Symposium* 2, 491-496

Grigg, R., (1998). Holocene coral reef accretion in Hawaii: a function of wave exposure and sea level history. *Coral Reefs* 17, 263-272

Hamylton, S., Spencer, T., (2011). Geomorphological modelling of tropical marine landscapes: Optical remote sensing, patches and spatial statistics. *Continental Shelf Research* 31, S151–S161

Harris, P., Purkis, S., Ellis, J. (2011). Analyzing Spatial Patterns in Modern Carbonate Sand Bodies From Great Bahama Bank. *Sedimentary Research* 81, 185-206

Hoeke, R., Storlazzi, C., Ridd, P., (2011), Hydrodynamics of a bathymetrically complex fringing coral reef embayment: Wave climate, in situ observations, and wave prediction. *Geophysical Research* 116, 1-20

Hongo, C., Kayanne, H., (2009). Holocene coral reef development under windward and leeward locations at Ishigaki Island, Ryukyu Islands, Japan. *Sedimentary Geology* 214, 62–73

Hongo,C., Kayanne, H., (2009). Holocene coral reef development under windward and leeward locations at Ishigaki Island, Ryukyu Islands, Japan. *Sedimentary Geology* 214, 62–73

Kan, H., (1995). Typhoon effects on sediment movement on reef edges and reef slopes. In: Bellwood, O., et al. (eds) Recent advances in marine science and technology (1994). Pacon International and James Cook University, Townsville, 191-201

Kan, H., Hori, N., Ichikawa, K., (1997) Formation of a coral reef-front spur. *Coral Reefs* 16, 3-4

Kan, H., Hori, N., Nakashima, Y., Ichikawa, K., (1995). Narrow reef flat formation in a high-latitude fringing reef. *Coral Reefs* 14, 123-130

Kench, P., Brander, R., Parnell, K., McLean, R., (2006). Wave energy gradients across a Maldivian atoll: Implications for island geomorphology. *Geomorphology* 81, 1-17

Kench, P., Brander, R., Parnell, K., O'Callaghan, J., (2009). Seasonal variations in wave characteristics around a coral reef island, South Maalhosmadulu atoll, Maldives. *Marine Geology* 262, 116-129

Kennedy, D., Woodroffe, C., (2002). Fringing reef growth and morphology: a review. *Earth Science Reviews*, 57, 255-277

Lidz, B., (2004). Coral reef complexes at an atypical windward platform margin: Late Quarternary, Southeast Florida. *Geological Society of America Bulletin*, 116, 974-988

Machado, G., Marfurt, K., Davogustto, O., Pranter, M. (2013). Seismic imaging of spur and groove structures in the San Andres Formation, Midland Basin, Texas. *SEG Houston Annual Meeting*, 1545-1549

Mandelier, P., Kench, P., (2012a). Analytical modelling of wave refraction and convergence on coral reef platforms: Implications for island formation and stability. *Geomorphology* 159-160, 84-92

Mandlier, P., (2012b). Field observations of wave refraction and propagation pathways on coral reef platforms. *Earth Surface Processes and Landforms* 38, 913-925

Mandlier, P.,Kench, P.(2012). Analytical modelling of wave refraction and convergence on coral reef platforms: Implications for island formation and stability. *Geomorphology* 159-160, 84–92

Mumby, P., Skirving, W., Strong, A., Hardy, J., LeDrew, E., Hochberg, E., Stumpf, R., David, L. (2004). Remote Sensing of coral reefs and their physical environment. *Marine Pollution Bulletin* 48, 219-228

Munk, W., Sargent M., (1948). Adjustment of Bikini Atoll to ocean waves. *Transcript: American Geophysics Union* 29, 855-860

O'Leary, M., Perry, C., (2010). Holocene reef accretion on the Rodrigues carbonate platform: An alternative to the classic "bucket-fill" model. *Geology* 38, 855-858

Perry, C., Kench, P., Smithers, S., Bernhard R., Yamano, H., O'Leary, M., (2011) Implications of reef ecosystem change for the stability and maintenance of coral reef islands. *Global Change Biology* 17, 3679-3696

Pomar, L, (2001). Types of carbonate platforms: a genetic approach. *Basin Research* 13, 313-334

Purkis, S., Riegl, B., Andrefouet, S., (2005). Remote Sensing of Geomorphology and Facies Patterns on a Modern Carbonate Ramp (Arabian Gulf, Dubai, U.A.E.) *Sedimentary Research* 75, 861-876

Purkis, S., Kohler, K., Riegl,B., Rohmann, S., (2007) The Statistics of Natural Shapes in Modern Coral Reef Landscapes. *Geology,* 155, 493-508

Rankey, E., Enos, P., Steffen, K., Druke, D., (2004). Lack of impact of hurricane Michelle on tidal flats, Andros Island, Bahamas: Integrated remote sensing and field Observations. *Sedimentary Research* 74, 654-661

Rankey, E., Doolittle, D., (2012). Geomorphology of carbonate platform-marginal uppermost slopes: Insights from a Holocene analogue, Little Bahama Bank, Bahamas. *Sedimentology* 59, 2146-2171

Rankey, E., Guidry, S., Reeder, S., Guarin, H. (2009) Geomorphic and Sedimentologic Heterogeneity Along Holocene Shelf Margin: Caicos Platform. *Sedimentary Research* 79, 440-456

Roberts, H., (1974) Variability of Reefs with Regard to Changes in Wave Power Around an Island. *Proceedings of the 2nd International Coral Reef Symposium* 2

Roberts, H., Murray, S., Suhayda,.N., (1975) Physical processes in a fringing reef system. *Marine Research* 33, 233-260

Rogers, J., Monismith, S., Feddersen, F., Storlazzi, C., (2013). Hydrodynamics of spur and groove formations on a coral reef. *Geophysical Research: Oceans* 118, 1-15

Rooney, J., Wessel, P., Hoeke, R., Weiss, J., Baker, J., Parrish, F., Fletcher, C., Chojnacki, J., Garcia, M., Brainard, R., Vroom, P., (2008). *Geology and geomorphology of coral reefs in the northwestern Hawaiian Islands. In: Riegl, B., Dodge, R. (eds) Coral Reefs of the USA. Coral Reefs of the World,* 1, 515-567

Ruiz de Alegria-Arzaburu, A., Marino-Tapia, I., Enrique, C., Silva, R., Gonzalez Leija, M., (2013) The role of fringing coral reefs on beach morphodynamics. *Geomorphology* 198, 69-83

Shaked, Y., Lazar, B., Marco, S.,Stein, M., Tchernov, D., Agnon, A. (2005). Evolution of fringing reefs: space and time constraints from the Gulf of Aqaba. *Coral Reefs* 24, 165-172

Shannon, A., Power, H., Webster, J., Vila-Concejo, A., (2012) Evolution of coral rubble deposits on a reef platform as detected by remote sensing. *Remote Sensing* 5, 1-18

Shinn, E., (1963). Spur and groove formation on the Florida reef tract. *Sedimentary Petrology*, 33, 291-303

Shinn, E., Hudson, J., Halley, R., Lidz, B., (1977). Topographic control and accumulation rate of some Holocene coral reefs: south Florida and Dry Torugas. *Proceedings at 3rd International Coral Reef Symposium* 2, 1-7

Shinn E., Hudson J., Robbin D., Lidz, B., (1981). Spurs and grooves revisited: construction versus erosion Looe Key Reef, Florida. *Proceedings at 4th International Coral Reef Symposium* 1, 475-483

Skarke, A., Trembanis, A., (2011). Parameterization of bedform morphology and defect density with fingerprint analysis techniques. *Continental Shelf Research* 31, 1688-1700

Sneh, A., Friedman, G., (1980). Spur and groove patterns on the reefs of the northern gulf of the Red Sea. *Sedimentary Petrology* 50, 981-986

Warrlich, G., Bosence, D., Waltham, D. (2005). 3D and 4D controls on carbonate and depositional systems: sedimentological and sequence stratigraphic analysis of an attached carbonate platform and atoll (Miocene, Nijar Basin, SE Spain). *Sedimentology* 52, 363-389

Windfinder. 2013, https://www.windfinder.com/

Wisuki. 2013, http://wisuki.com/

Wood, R., Oppenheimer, C., (2000). Spur and groove morphology from a Late Devonian reef. *Sedimentary Geology* 133, 185-193

Yamano, H., Abe, O., Matsumoto, E., Kayanne, H., Yonekura, N., Blanchon, P., (2003) Influence of wave energy on Holocene coral reef development: an example from Ishigaki Island, Ryukyu Islands, Japan. *Sedimentary Geology* 159, 27-41

Yamano, H., Shimazaki, H., Matsunaga, T., Ishoda, A., McClennen, C., Yokoki, H., Fujita, K., Osawa, Y., Kayanne, H. (2006). Evaluation of various satellite sensors for waterline extraction in a coral reef environment: Majuro Atoll, Marshall Islands. *Geomorphology* 82, 398-411

# Appendix A

Compiled Current Data for each of the nine sites of this study. Table shows site name, year, month, and the averaged direction in degrees the currents were flowing.

| Cook Reef | Year | Month | Direction (Degrees) | | Year | Month | Direction (Degrees) |
|---|---|---|---|---|---|---|---|
| | 2006 | 1 | 20 | | 2008 | 1 | 320 |
| | 2006 | 3 | 70 | | 2008 | 3 | 340 |
| | 2006 | 6 | 210 | | 2008 | 6 | 320 |
| | 2006 | 8 | 280 | | 2008 | 8 | 150 |
| | 2006 | 10 | 190 | | 2008 | 10 | 200 |
| | 2006 | 12 | 80 | | 2008 | 12 | 160 |
| | | | | | | | |
| Foa and Lafuka | Year | Month | Direction (Degrees) | | Year | Month | Direction (Degrees) |
| | 2006 | 1 | 160 | | 2008 | 1 | 170 |
| | 2006 | 3 | 210 | | 2008 | 3 | 180 |
| | 2006 | 6 | 180 | | 2008 | 6 | 200 |
| | 2006 | 8 | 20 | | 2008 | 8 | 175 |
| | 2006 | 10 | 165 | | 2008 | 10 | 30 |
| | 2006 | 12 | 170 | | 2008 | 12 | 10 |
| | | | | | | | |
| Palmerston | Year | Month | Direction (Degrees) | | Year | Month | Direction (Degrees) |
| | 2006 | 1 | 90 | | 2008 | 1 | 300 |
| | 2006 | 3 | 260 | | 2008 | 3 | 190 |
| | 2006 | 6 | 300 | | 2008 | 6 | 230 |
| | 2006 | 8 | 290 | | 2008 | 8 | 270 |
| | 2006 | 10 | 240 | | 2008 | 10 | 345 |
| | 2006 | 12 | 280 | | 2008 | 12 | 110 |
| | | | | | | | |
| Aitutaki | Year | Month | Direction | | Year | Month | Direction |
| | 2006 | 1 | 195 | | 2008 | 1 | 310 |
| | 2006 | 3 | 245 | | 2008 | 3 | 100 |
| | 2006 | 6 | 227 | | 2008 | 6 | 180 |
| | 2006 | 8 | 60 | | 2008 | 8 | 20 |
| | 2006 | 10 | 270 | | 2008 | 10 | 270 |
| | 2006 | 12 | 300 | | 2008 | 12 | 90 |

| Motu One | Year | Month | Direction (Degrees) | | Year | Month | Direction (Degrees) |
|---|---|---|---|---|---|---|---|
| | 2006 | 1 | 220 | | 2008 | 1 | 120 |
| | 2006 | 3 | 190 | | 2008 | 3 | 70 |
| | 2006 | 6 | 230 | | 2008 | 6 | 200 |
| | 2006 | 8 | 290 | | 2008 | 8 | 300 |
| | 2006 | 10 | 250 | | 2008 | 10 | 270 |
| | 2006 | 12 | 210 | | 2008 | 12 | 300 |
| | | | | | | | |
| Mauhippa | Year | Month | Direction (Degrees) | | Year | Month | Direction (Degrees) |
| | 2006 | 1 | 285 | | 2008 | 1 | 30 |
| | 2006 | 3 | 85 | | 2008 | 3 | 145 |
| | 2006 | 6 | 120 | | 2008 | 6 | 270 |
| | 2006 | 8 | 70 | | 2008 | 8 | N/A |
| | 2006 | 10 | 180 | | 2008 | 10 | 60 |
| | 2006 | 12 | 115 | | 2008 | 12 | 10 |
| | | | | | | | |
| | Year | Month | Direction (Degrees) | | Year | Month | Direction (Degrees) |
| Tenarunga | 2006 | 1 | 230 | | 2008 | 1 | 330 |
| | 2006 | 3 | 325 | | 2008 | 3 | 210 |
| | 2006 | 6 | 315 | | 2008 | 6 | 120 |
| | 2006 | 8 | 200 | | 2008 | 8 | 310 |
| | 2006 | 10 | 260 | | 2008 | 10 | 160 |
| | 2006 | 12 | 90 | | 2008 | 12 | 335 |
| | | | | | | | |
| | Year | Month | Direction (Degrees) | | Year | Month | Direction (Degrees) |
| Bajo Nuevo | 2006 | 1 | 320 | | 2008 | 1 | 305 |
| | 2006 | 3 | 330 | | 2008 | 3 | 20 |
| | 2006 | 6 | 340 | | 2008 | 6 | 310 |
| | 2006 | 8 | 20 | | 2008 | 8 | 25 |
| | 2006 | 10 | 300 | | 2008 | 10 | N/A |
| | 2006 | 12 | 360 | | 2008 | 12 | 245 |
| | | | | | | | |
| | Year | Month | Direction (Degrees) | | Year | Month | Direction (Degrees) |
| Diego Garcia | 2006 | 1 | 340 | | 2008 | 1 | 290 |
| | 2006 | 3 | 340 | | 2008 | 3 | 120 |
| | 2006 | 6 | 340 | | 2008 | 6 | 170 |
| | 2006 | 8 | 220 | | 2008 | 8 | 190 |
| | 2006 | 10 | 190 | | 2008 | 10 | 250 |
| | 2006 | 12 | 290 | | 2008 | 12 | 290 |